Zeitschrift: Helvetica Physica Acta
Band: 37 (1964)
Heft: II

Artikel: Absorption spectra of Uranium (IV) in octahedral coordination
Autor: Pappalardo, R. / Jørgensen, C.K.
DOI: https://doi.org/10.5169/seals-113473

Absorption Spectra of Uranium (IV) in Octahedral Coordination

by **R. Pappalardo** and **C. K. Jørgensen**

Cyanamid European Research Institute, Cologny (Geneva), Switzerland

(15.VIII.63)

Summary. Optical absorption spectra of crystals containing octahedrally coordinated U^{4+} ions in triphenylphosphonium complex salts are reported for the region 2.5 μ to 0.3 μ, both at RT and 78° K. Vibrational frequencies for the $\langle UCl_6\rangle^{2-}$ and $\langle UBr_6\rangle^{2-}$ groups have been found superimposed on to the electronic transitions. General properties of the spectra in connection with the $5f^2$-energy levels are discussed.

1. Introduction

The excited electronic levels within 3 d^n-systems can be characterized in solids by a predominant crystal-(or ligand) field[1)2)3)], on to which spin-orbit interactions can be added as higher-order perturbations. The analogous excited electronic levels in 4 f^n-systems are determined primarily by spin-orbit effects[2)3)4)], on to which crystal-field effects act as perturbations.

On the contrary, for the case of 5 f^n-systems, it seems that crystal-field and spin-orbit effects must be treated simultaneously in a perturbation calculation. This accounts for the fact that the detailed interpretation of optical transitions within 5 f^n-shells is still in its initial stage[5)6)].

Another handicap for the identification of the excited 5 f^n-levels has been the dearth of detailed studies, especially optical spectra, of 5 f^n-systems in highly symmetric coordinations, where the problems of interpretation are relatively easier. Important progress towards a satisfactory solution of the problem has followed from the recent work by SATTEN and co-workers on octahedrally coordinated uranium(IV) in chloride complex salts[7)8)].

In what follows we report spectra of octahedrally coordinated U^{4+} in crystals of bromide and chloride triphenylphosphonium complex salts. We hope that the data will confirm and supplement some of the conclusions reached by SATTEN and co-workers[7)8)] and contribute towards the identification of the electronic 5 f^n-levels.

2. Experimental

The U^{4+} ion is usually coordinated by six or more neighbouring ions, very frequently located in such a way that the point symmetry at the U^{4+} site is very low. Octahedrally coordinated $\langle UCl_6\rangle^{2-}$ and $\langle UBr_6\rangle^{2-}$, as many other complex ions, exist in solutions and in the solid state, provided they are stabilized by large cations. So the

detailed studies by SATTEN and coworkers[7][8]) have been performed on crystals of Cs_2UCl_6; $[N(C_2H_5)_4]_2\,UCl_6$ and $[N(CH_3)_4]_2\,UCl_6$. The corresponding bromide salts were found to be not stable enough for low-temperature studies of crystal spectra.

Recently DAY and VENANZI[9]) and also ALLISON and MANN[10]) discussed the stabilization of $\langle MCl_6\rangle^{2-}$ and $\langle MBr_6\rangle^{2-}$ groups, in the presence of the triphenylphosphonium cation $[P\,\phi_3\,H]^+$ (where ϕ stands for $-C_6H_5$). The complex triphenylphosphonium salts[11]) of $\langle UCl_6\rangle^{2-}$ and $\langle UBr_6\rangle^{2-}$ extracted by organic solvents can be crystallized from acetonitrile and/or nitromethane solutions, and are remarkably stable.

Spectrophotometric studies of solutions of $[P\,\phi_3\,H]_2UCl_6$; $[P\,\phi_3\,H]_2UBr_6$ and $[P\,\phi_3\,H]_2U(Br, Cl)_6$ have been recently reported by JØRGENSEN[11]).

Here we report some preliminary studies of the corresponding crystals of $[P\,\phi_3\,H]_2UCl_6$; $[P\,\phi_3\,H]_2UBr_6$ and also of the mixed crystals $[P\,\phi_3\,H]_2$ (Sn, U)Cl_6 and $[P\,\phi_3\,H]_2$ (Sn, U)Br_6, since the uranium salts easily form mixed salts with the corresponding tin triphenylphosphonium salts. The morphological habits of the emerald green $[P\,\phi_3\,H]UCl_6$ crystals are as follows: thin and long prismatic rods, or flattened rhombohedra, or finally flat plates showing a nice trigonal symmetry. Two of the habits of growth correspond to two different types of spectra. The crystals from $[P\,\phi_3\,H]_2$ (Sn, U)Cl_6 show a rhombohedric habit, and only one type of absorption spectrum.

Table I.

Data for some of the samples used. Relevant spectra in Figure 1 to Figure 25

Sample	Composition	Thickness	Density
A 1	$[P\,\phi_3H]_2\ UBr_6$	1 mm	
A 2	$[P\,\phi_3H]_2\ UBr_6$	0·5 mm	1·848
B 1	$[P\,\phi_3H]_2$ (Sn, U) Br_6*)	0·5 mm	1·797
B 2	$[P\,\phi_3H]_2$ (Sn, U) Br_6*)	0·5 mm	1·788
F 5	$[P\,\phi_3H]_2$ (Sn, U) Br_6*)	0·9 mm	1·783
J 4	$[P\,\phi_3H]_2$ (Sn, U) Br_6*)	0·8 mm	
A 5	$[P\,\phi_3H]_2\ Sn\ Br_6$	1·1 mm	1·730
F 7	$[P\,\phi_3H]_2\ Sn\ Br_6$	0·55 mm	1·739
A 3	$[P\,\phi_3H]_2\ UCl_6$	0·95 mm	1·645
A 4	$[P\,\phi_3H]_2\ UCl_6$	0·75 mm	1·644
F 6	$[P\,\phi_3H]_2\ UCl_6$	0·6 mm	1·664
B 3	$[P\,\phi_3H]_2$ (Sn, U) Cl_6**)	1·0 mm	1·645
F 4	$[P\,\phi_3H]_2$ (Sn, U) Cl_6**)	0·65 mm	1·634

*) From equimolecular solutions of $[P\,\phi_3H]_2\ SnBr_6$ and $[P\,\phi_3H]_2\ UBr_6$.
**) From equimolecular solutions of $[P\,\phi_3H]_2\ SnCl_6$ and $[P\,\phi_3H]_2\ UCl_6$.

The $[P\,\phi_3\,H]_2UBr_6$ crystals grow as prismatic rods. Both the indiluted $\langle UBr_6\rangle$ salts and those diluted in tin show the same type of absorption spectra. Yellow $[P\,\phi_3\,H]_2\ SnBr_6$ crystals can be grown easily from solutions and can reach dimensions of the order of 1 cm. The density of the crystals was found by flotation in tetrabromoethane/benzine mixtures (Table I). The crystal crops from the equimolecular

solutions of tin/uranium salts contain essentially a single phase. So the corresponding crystals of mixed salts should have an approximately equal content in tin and uranium. This can be seen from the density of the samples.

Spectra at room temperature and 78° K were taken on a Cary 14 Universal Spectrophotometer in the regiom 2·5 μ to $\sim$ 0·3 μ. Spectra were also taken in the 15 μ to 25 μ region on a Perkin-Elmer Infracord. The absorption of the organic cation interferes seriously with the detection of U^{4+} absorptions the latter region. Data on the samples used are to be found in Table I. Spectra were also taken using light polarized by Glen-Thompson prisms, in order to see if any anisotropic absorption took place. Such effect, though present, are not very pronounced in the samples used so far. Finally, some of the crystals we studied were not large enough to use the Cary 14 Spectrophotometer in such a way to obtain the maximum possible resolution. For this reason we indicate esplicitly in the photometric tracings to follow what the operating slit-widths were, in mm units.

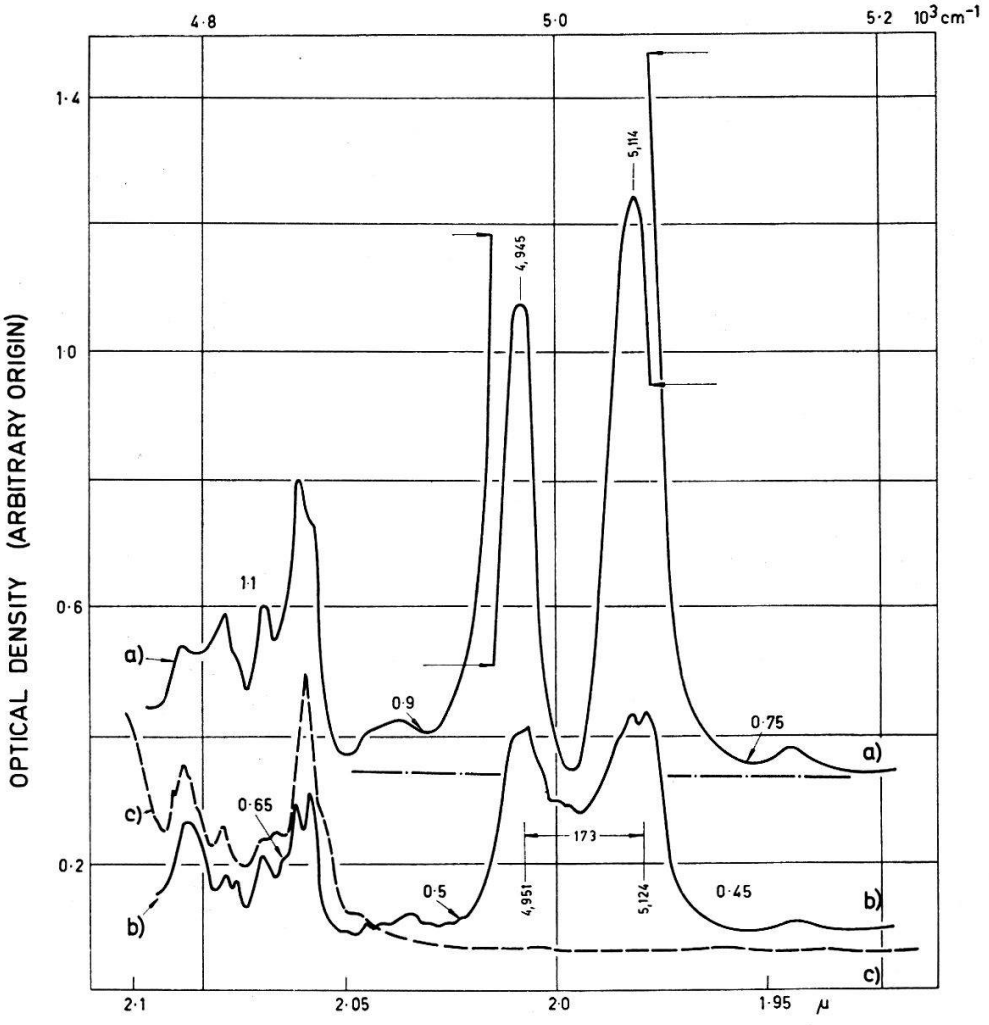

Figure 1

a) $[P\phi_3H]_2$ (Sn, U)Cl_6, sample F4 at room temperature. Thickness 0·65 mm; b) same at 78° K; c) $[P\phi_3H]_2$ $SnBr_6$ at RT, sample F7. Thickness 0·55 mm. In curve a) the base-line is shifted, in order to keep the intense peaks within the figure. Note the marked decrease in intensity at low temperatures. Numbers on the curves indicate slit-widths in mm. The peak separation ($\sim$173 cm^{-1}) is close to twice the 'ungerade' frequency Γ_{5u} of 80 cm^{-1} (see text).

3. The observed spectra

The U^{4+} ion with electronic configuration (Rn)$5f^2$ absorbs in over 20 regions of the spectrum from 2·5 μ to 0·3 μ, each of these absorptions showing complex fine structure at 78° K and RT. Some of the lines are very sharp even at RT and resemble the typical absorption lines of rare-earth ions. The large number of absorption lines in U^{4+} raises the problem of how to report briefly the observed spectra. A tabulation of all lines would be too lengthy. A collection of the photometric tracings at low scanning speed, though lengthy too, possibly condenses to advantage a large number of useful data, such as position, absolute and relative intensity of lines, their temperature shifts and how groups shift in going from $\langle UCl_6\rangle^{2-}$ to $\langle UBr_6\rangle^{2-}$. All these data are valuable to clarify the fine structure of each group, so as to locate the electronic levels and ultimately the values of the crystal field parameters. Oscillator strength values can also be derived from the photometric tracings and from the data of Table I. We indicate here some typical values of oscillator strengths. The third peak of group P, at $\sim$ 16,230 cm^{-1} (Figure 18a) has $f \sim 6 \cdot 10^{-7}$. In Figure 4a, the peak at 4,916 cm^{-1} has $f \sim 3 \cdot 10^{-5}$. The values are obtained assuming an equimolecular content in $\langle UX_6\rangle^{2-}$ and $\langle SnX_6\rangle^{2-}$.

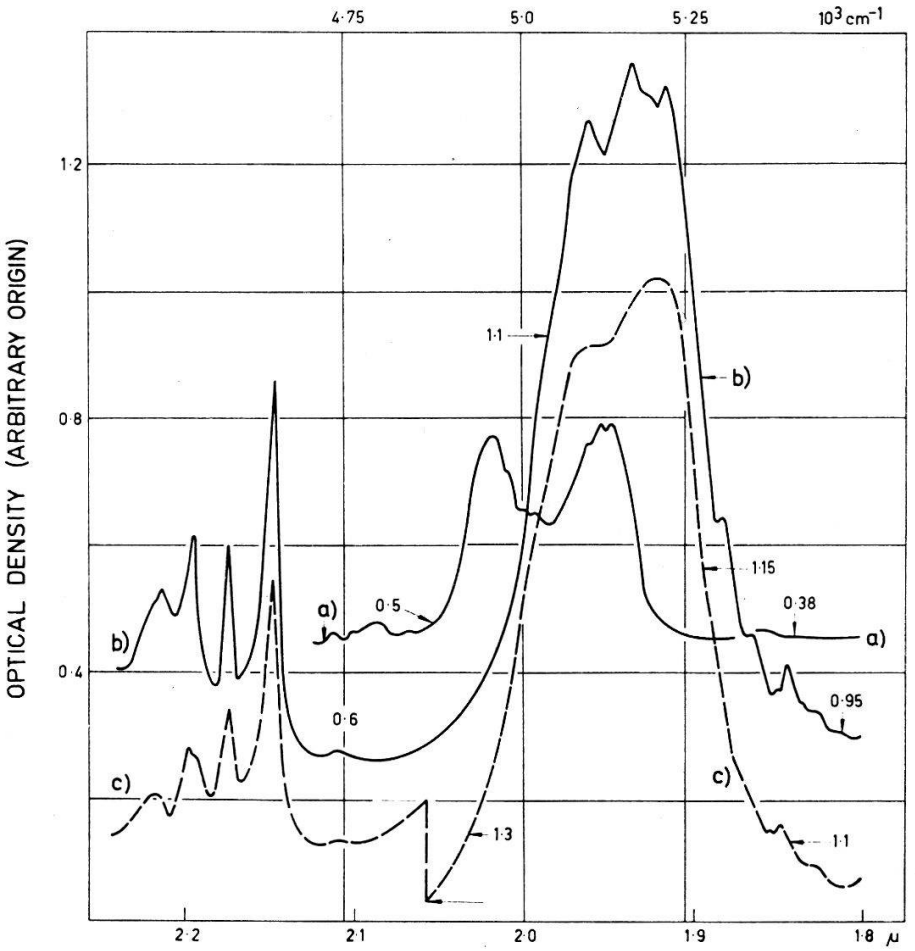

Figure 2

a) $[P\phi_3H]_2$ (Sn, U)Cl_6, sample F4, at 78° K; b) $[P\phi_3H]_2$ UCl_6, sample F6 at 78° K. Thickness 0·6 mm; c) same, at RT. There is a base-line shift in curve c) between 2·0 and 2·1 μ, to avoid overlap with curve b). By comparison with Figure 1, the intensity decrease at low temperature is much less pronounced.

The number of absorption data is further increased by the fact, already mentioned, that two types of spectra are found for the $\langle UCl_6\rangle^{2-}$ group. One such spectrum, shown by the mixed tin-uranium crystals and by the trigonal $[P\,\phi_3\,H]_2UCl_6$, resembles the spectra reported by Satten and alii for Cs_2UCl_6, the tetramethylammonium and tetraethylammonium complex chlorides. We shall label it $\langle UCl_6\rangle^{2-}_{reg}$, since the complex anion forms a regular octahedron. The other type of spectrum we shall associate to a group $\langle UCl_6\rangle^{2-}_{dist}$, probably a distorted octahedron. Some spectra of $[P\,\phi_3\,H]_2\,SnBr_6$ crystals are shown for the regions where the organic cation absorbs too.

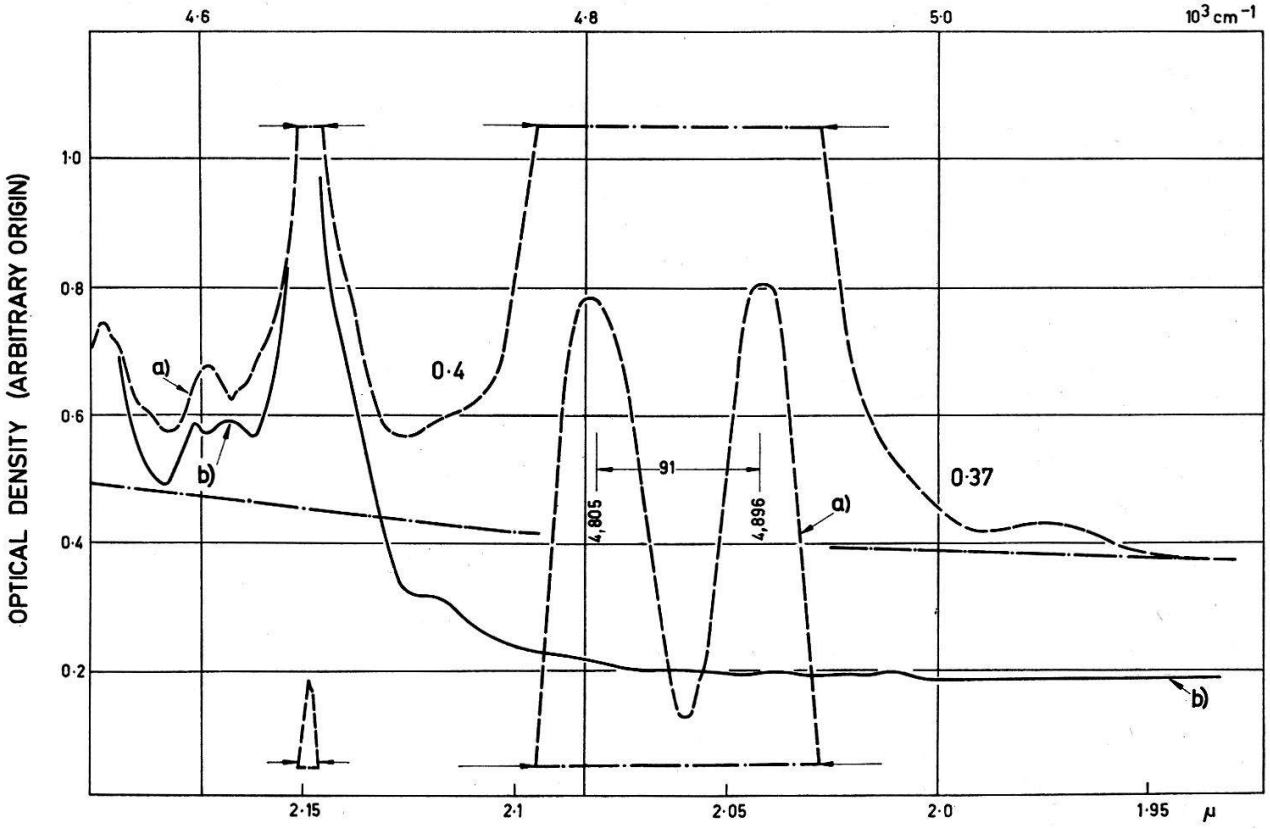

Figure 3

a) $[P\,\phi_3H]_2$ (Sn, U)Br_6, sample F5 at RT. Thickness 0·9 mm; b) $[P\,\phi_3H]_2\,SnBr_6$, sample A5, at RT. Thickness 1·1 mm. The peak separation of 91 cm^{-1}, is to be compared to the separation of 173 cm^{-1} for $[P\,\phi_3H]_2$ (Sn, U)Cl_6 in Figure 1.

The best photometric tracings for the infrared region and for the visible/near ultraviolet region pertain to two different sets of samples. For considerations of relative intensities of the various absorption groups in the same complex ion $\langle MX_6\rangle^{2-}$, the group at $\sim$ 6700 Å is given for both sets of samples.

4. General properties of the spectra

First of all our contention that the spectra are due to octahedral $\langle UX_6\rangle^{2-}$ groups is supported by the close similarity of the $\langle UCl_6\rangle^{2-}_{reg}$ spectra when compared with those of Ref. 7 and 8. The macroscopic symmetry of the crystals containing $\langle UCl_6\rangle^{2-}_{dist}$ may not be cubic, but the point symmetry around U^{4+} can still be predominantly

octahedral, such as found for trigonal Cs_2UCl_6 and orthorhombic $[N(C_2H_5)_4]_2\,UCl_6$, the spectra of which closely reproduce[7][8]) those of cubic $[N(CH_3)_4]_2\,UCl_6$. The $\langle UBr_6\rangle^{2-}$ spectra are also consistent with the assumption of $\langle UBr_6\rangle^{2-}$ octahedra, because they are analogous to the $\langle UCl_6\rangle^{2-}_{reg}$ spectra shifted by appropriate amounts.

The preliminary analysis by SATTEN et alii[7][8]) of the spectra of U^{4+} emphasized the following points.

a) The transitions are mostly vibronic, namely vibrational quanta accompany the pure electronic transitions, otherwise forbidden for a U^{4+} ion located in a site possessing a center of inversion. The position of the electronic levels so inferred is reported here in Table II, Columns 2, 3, 4.

Table II

Position at 78° K of electronic levels of U^{4+}
(the lines in parenthesis are vibronically located)

Term label	Cs_2UCl_6[a)b)]	$[N(CH_3)_4]_2 \cdot UCl_6$[a)b)]	$[N(C_2H_5)_4]_2 \cdot UCl_6$[b)]	$[P\phi_3H]_2 \cdot (Sn, U)Cl_6$	$\langle UCl_6\rangle_{dist}$	$[P\phi_3H]_2 \cdot (Sn, U)Br_6$
A	(5,046)[c)]	–		(5,037)		(4,870)
B	(6,282)[c)]	–		(6,342)		
C	(7,273)[c)]	–				
D	(8,158)[c)]	–		(8,152)		
E	(9,232)	(9,237)		(9,196)		(8,981)
F	(9,540)	(9,612)		(9,578)		(9,216)
G	(10,065)	(10,069)		(10,025)		(9,783)
H	(11,176)	(11,200)		(11,010)	11,398	(10,950)
I	12,128·1	12,128·9	12,122·1	(12,102)	12,322	(11,798)
J	(12,878·0)	12,860·7	12,856·2			
K	(12,984·0)	12,968·5	12,908·0		13,157	
L	14,789·0	14,835·3	14,863·5	(14,824)	14,892	(14,876)
M	15,213·0	15,234·1	15,231·2	(15,200)		(15,368 ?)
N	15,674·4	15,719·8	(15,730·0)	(15,735)		(15,400 ?)
O	(15,754·3)	(15,775·3)	(15,785·0)			
P	16,797·1	16,834·6	16,817·8	(16,790)	(17,205)	(16,159)
Q	18,822·6	(18,870·0)	18,807·3	(18,776)	19,286	(18,160)
R	(20,484)	(20,592·8)	(20,490·0)	(18,838)		
S	(20,760 ?)	(20,753 ?)				
T	21,814·4	21,898·7	21,896·1	(22,000)		(21,297)
U	22,183·0	22,229·0	22,233·3			
V	23,398·6	23,446·5	(23,402·3)			
W	(24,700·0)	(24,738·8)	(24,669·0)	(24,680)		(23,960)

[a)] SATTEN, YOUNG and GREEN, J. Chem. Phys. *33*, 1140 (1960).
[b)] S. A. POLLACK and R. A. SATTEN, J. Chem. Phys. *36*, 804 (1962).
[c)] At Room Temperature.

b) Of the possible vibrational frequencies, the three 'ungerade' frequencies of the $\langle MX_6\rangle$ complexes are considered responsible for the most intense transitions observed,

occurring for $\langle UCl_6 \rangle$ at distances[8]) 80 cm^{-1} (Γ_{5u}); 114 cm^{-1} (Γ_{4u}) and 260 cm^{-1} (Γ_{4u}) from the position of the pure electronic transitions. Apart from these frequencies, the photographic technique and the very low temperatures used in Ref. 7 and 8 made it possible to find a large number of other, less intense, vibrational frequencies associated with the electronic transitions. High vibrational frequencies (> 900 cm^{-1}) found[7])[8]) superimposed on to the most intense vibronic transitions are associated with the vibrational frequencies of the complex cations.

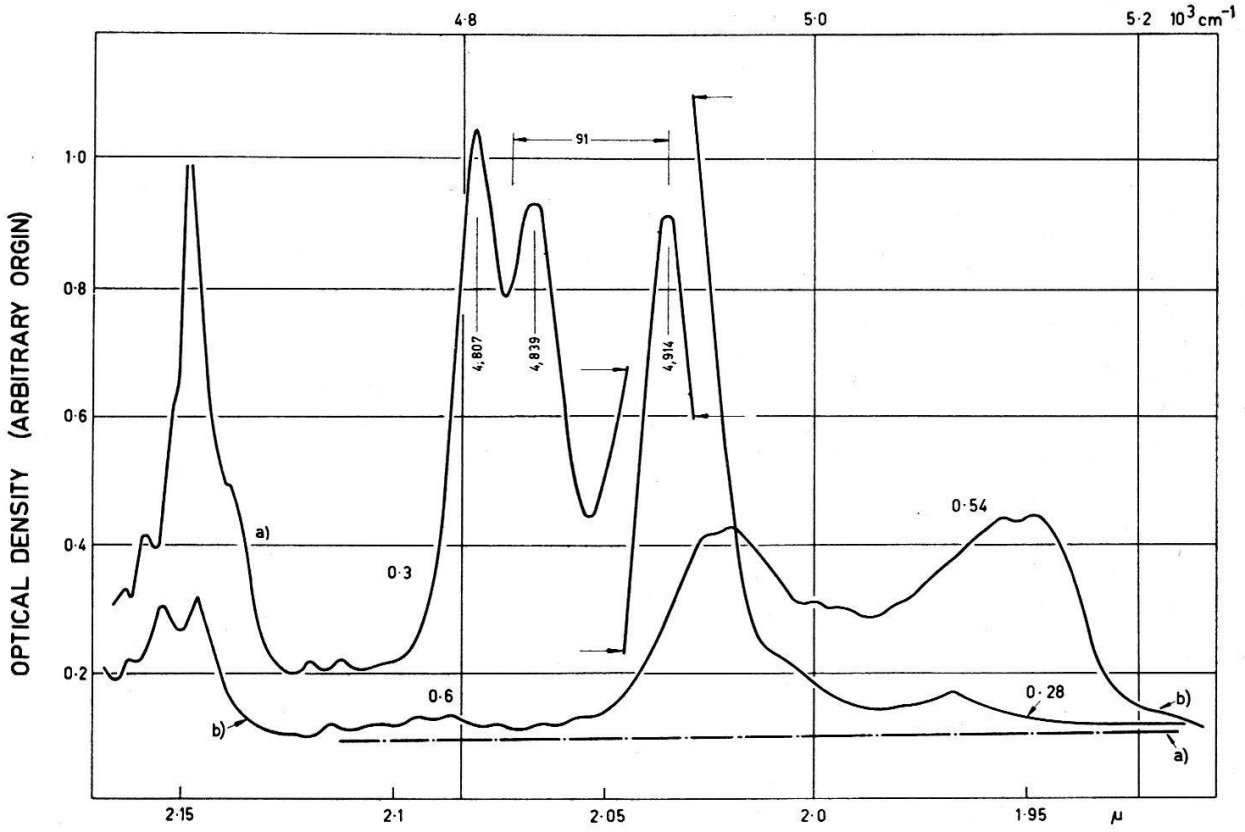

Figure 4

a) $[P\phi_3H]_2$ (U, Sn)Br_6, sample F 5 at 78° K; b) $[P\phi_3H]_2$ (U, Sn)Cl_6, sample F 4 at 78° K; comparison of a) with Figure 3, shows a marked temperature decrease and pronounced splitting in the low-frequency component of the Room-Temperature doublet. This is consistent with a 'pure' electronic transition at ~ 4870 cm^{-1}.

c) The absence of some of the intense 'ungerade' vibrations in a given transition, can be used to infer the symmetry character of the excited electronic level involved, assuming, from magnetic susceptibility data[12]) the groundstate to be of the symmetry type Γ_1 and making use of the selection rules:

$$\begin{aligned} &\text{for } \Gamma_{4u} \text{ modes} \quad \Gamma_1 \longleftrightarrow \Gamma_2 \\ &\text{for } \Gamma_{5u} \text{ modes} \quad \Gamma_1 \longleftrightarrow \Gamma_1 \end{aligned} \tag{1}$$

In detail the ~ 80 cm^{-1} vibration was found[7]) absent in the levels at

$$14{,}895;\ 16{,}836;\ 20{,}612 \text{ cm}^{-1} \tag{2}$$

and the 114 cm^{-1} and 260 cm^{-1} frequencies absent in the levels at

$$9{,}615;\ 10{,}071;\ 12{,}130;\ 24{,}749\ cm^{-1} \tag{3}$$

d) With the decrease in temperature most line groups shift to higher frequencies, with only one marked exception, the group at $\sim 14{,}800$ cm^{-1}. This behaviour is associated with the difference in the slope of the energy of ground and excited levels as function of the crystal field.

Accordingly, a first inspection of the spectra of Figure 1 to Figure 25 will be concerned with the following points.

a') The same number of intense line groups is found for $\langle UCl_6\rangle^{2}_{reg}$ and $\langle UBr_6\rangle^{2-}$. The same is generally true in comparing $\langle UCl_6\rangle_{dist}$ and $\langle UBr_6\rangle^{2-}$, although at least one additional group is found for $\langle UCl_6\rangle^{2-}{}_{dist}$ in the 0·7 μ to 0·6 μ region.

b') Simply on the basis of our data, a vibrational analysis of the fine structure as performed by SATTEN et alii[7][8] is quite unambiguous for at least two line groups:

group L (fig. 14, 15, 17) and group P (fig. 17, 18, 19).

In these two cases, after considering the temperature dependance of the line intensity, we find the following vibrational frequencies, where values in parenthesis are vibrational frequencies of the ground state.

$\langle UCl_6\rangle^{2-}_{reg}$	Group L	RT:	(27), 30 – (112), 112 – (255), 255	
	Group P	RT:	– (104), 104 – (256), 256	
	Group L	78° K:	(25), 28 – (114), 114 – (258), 260	
	Group P	78° K:	(21), 35 – (112), 112 – (256), 256	(4)
$\langle UBr_6\rangle^{2-}$	Group L	RT:	(72), 72 – (181), 177	
	Group P	RT:	(70), 71 – (183), 183	
	Group L	78° K:	(74), 74 – (186), 179	
	Group P	78° K:	(27), 23 – (75), 68 – (186), 185	

The other vibrational frequency[7][8] of ~ 80 cm^{-1} for $\langle UCl_6\rangle^{2-}$ is absent in these two groups, as expected from (1) and (2). The vibrational analysis ot the other groups is not so strikingly evident, at least at 78° K, and was used in the form of a working hypothesis to locate the position of the elctronic transitions listed in Table II. In a first approximation, where the force constants are left unchanged, the vibrational frequencies of the complex $\langle MX_6\rangle$ should be inversely proportional to the square root of the mass of X. The following ratios (5) and (6) compare favourably:

$$\left(\frac{\nu_{Cl}}{\nu}\right)_{Br\ \Gamma_{4u}} \simeq \frac{260}{180} = 1{\cdot}44\,; \quad \left(\frac{\nu_{Cl}}{\nu}\right)_{Br\ \Gamma_{4u}} \simeq \frac{114}{72} = 1{\cdot}58 \tag{5}$$

$$\left(\frac{M_{Br}}{M_{Cl}}\right)^{\frac{1}{2}} = 1{\cdot}5 \tag{6}$$

c') The absence of the ~ 80 cm^{-1} vibration of the chloride complex was also checked in our case for the groups L and P. The band at $\sim 20{,}600$ [see rel. (2) and

Figure 22a, b, c] is too broad at 78° K for one to be able to draw any conclusion. The absence of the ~ 114 cm^{-1} and 258 cm^{-1} vibration [rel. (3)] is checked for the groups at $\sim 5{,}040$ cm^{-1} (Fig. 1 and 2); 9,578 cm^{-1} (Figure 11); 10,025 cm^{-1} (Figure 11); 12,130 cm^{-1} (Figure 13) and 24,750 cm^{-1} (Figure 24).

d') As for the shifts of the individual line groups with temperature, since vibrational frequencies do not seem to change with temperature or in going from the ground state to the excited state (Figure 14, 15 and Figure 18, 19), we may generally consider in each group a given line and follow its behaviour with temperature. The line has to be fairly isolated, so as to avoid apparent shifts due to intensity changes of two overlapping lines. The data are collected in Table III. One of the pecularities of the spectra reported[7][8]) was the negative temperature shift of group L. We found a similar behaviour for such a group in $\langle UCl_6\rangle^{2-}$ but the temperature shift of group L in $\langle UBr_6\rangle^{2-}$ is positive.

Table III

Some typical temperature shifts (78° K–RT) of lines and groups (Columns 2 and 3) and energy separation at 78° K of baricenters of corresponding line groups in $\langle UCl_6\rangle^{2-}_{reg}$ and $\langle UBr_6\rangle^{2-}$.

Term label	$\langle UCl_6\rangle^{2-}_{reg}$	$\langle UBr_6\rangle^{2-}$	$\langle UCl_6\rangle^{2-}_{reg} - \langle UBr_6\rangle^{2-}$
A	+8	+18	+170
B	+8	+9	+135
C	?	?	+240
D	+20	+19	+280
E			
F	+4	+8	+280
G	+10	+10	+150
H	+5	+2	+155
I	+9	+15	+300
J	+20		+400
K			
L	−22[a])	+8	− 52[a])
M	+6		−168[a]) (?)
N			+335 (?)
O			
P	+41[a])	+36[a])	+631[a])
Q		+34	+480
R			
S			+370
T	+14	+70 (?)	+460
U	+31 (?)		
V			
W			

[a]) Considering here the electronic transition.

e') The $\langle UBr_6\rangle^{2-}$ spectra are shifted towards lower frequencies with respect to those of $\langle UCl_6\rangle^{2-}_{reg}$. The amount of the shift at 78° K (Table III) varies from a minimum

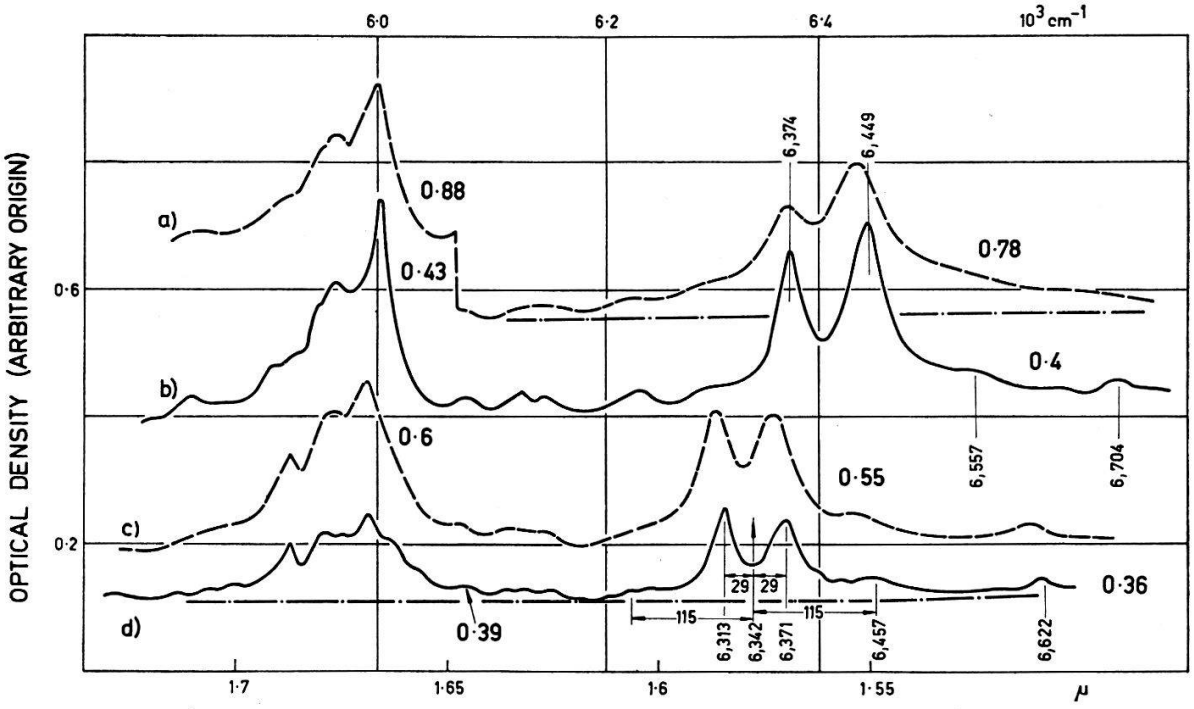

Figure 5

a) $[P\phi_3H]_2\ UCl_6$, sample F6 at RT; b) same at 78° K; c) $[P\phi_3H]_2$ (Sn, U)Cl_6, sample F4 at RT; d) same at 78° K. The absorption at $\sim 6000\ cm^{-1}$, common to all curves, is associated with the organic cation (see also Figure 6).

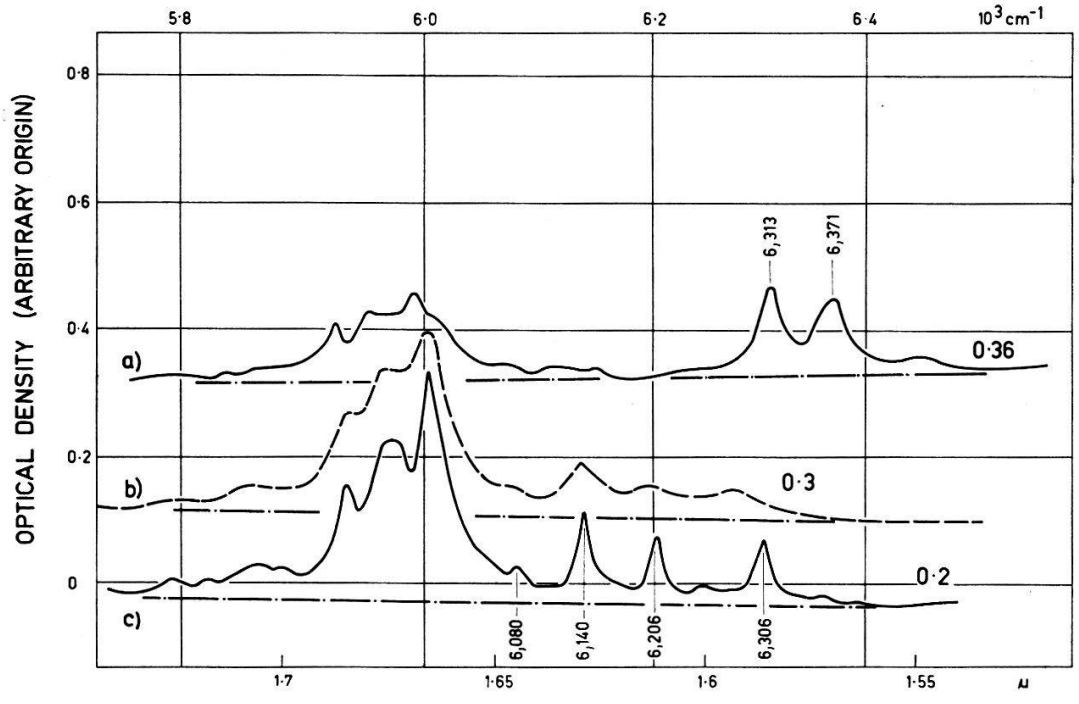

Figure 6

a) $[P\phi_3H]_2$ (Sn, U)Cl_6, sample F4 at 78° K; b) $[P\phi_3H]_2$ (Sn, U)Br_6 sample F5 at RT; c) same at 78° K.

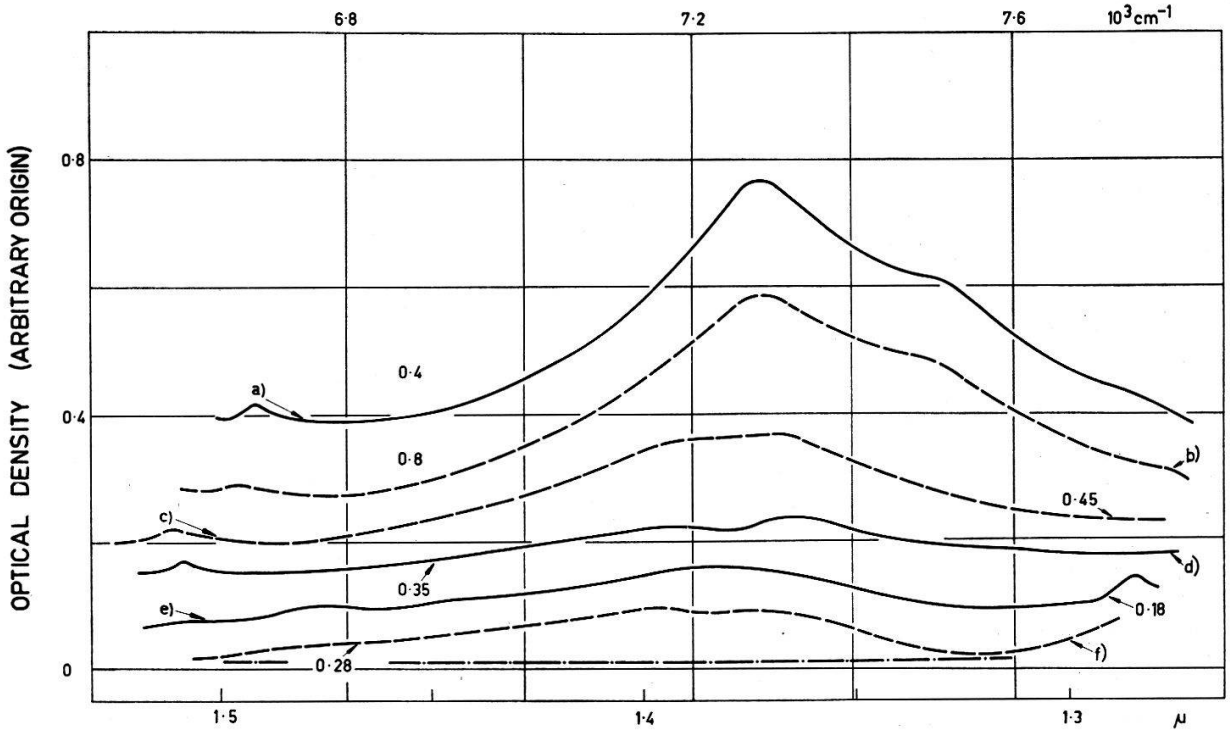

Figure 7

a) $[P\phi_3H]_2UCl_6$, sample F6 at 78° K; b) same at RT; c) $[P\phi_3H]_2(Sn, U)Cl_6$, sample F4 at RT; d) same at 78° K; e) $[P\phi_3H]_2(Sn, U)Br_6$, sample F5 at 78° K; f) same at RT. A similar broad, structurless band is found at $\sim$ 20,000 cm^{-1} (see Figure 22 and 23).

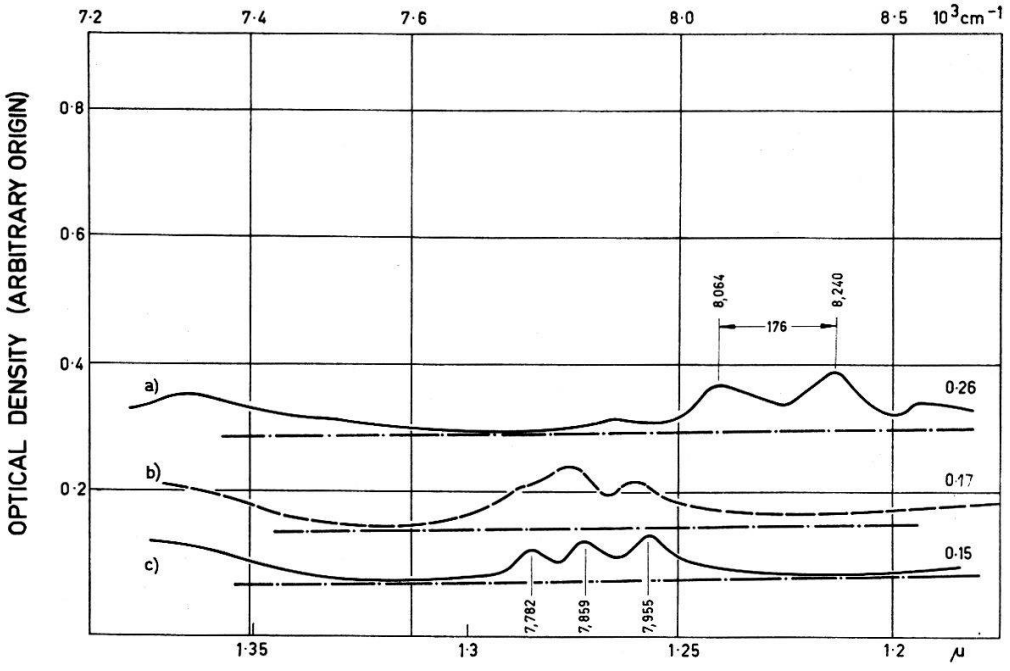

Figure 8

a) $[P\phi_3H]_2(Sn, U)Cl_6$, sample F4 at 78° K; b) $[P\phi_3H]_2(Sn, U)Br_6$, sample F5 at RT; c) same at 78° K. The doublet separation in a) is the same as found at $\sim$ 5000 cm^{-1} (Figure 1). The triplet of curve c) has exactly the same structure as the triplet of Figure 6, c).

of ~ 130 cm^{-1} to a maximum value of ~ 830 cm^{-1}. The only striking exception is the negative shift in the 15,000 cm^{-1} region. We shall return later to this point.

f') The spectrum of $\langle UCl_6 \rangle_{dist}$ is similar to the spectrum of $\langle UCl_6 \rangle_{reg}$, but shows shifts of the line groups to higher energies and different fine structure. The reasons suggesting that the $\langle UCl_6 \rangle_{dist}$ is due to U^{4+} in a distorted octahedral arrangement are as follows*. Vibrational frequencies of 260 cm^{-1} and 90 cm^{-1} are present (Figure 17); line groups L are similar in both systems (Figure 17), except for the appearance in $\langle UCl_6 \rangle_{dist}$ of the pure electronic transition (absence of a center of inversion?); the negative temperature (-17 cm^{-1}) shift of electronic transition L_e; similarity of groups P in both systems (Figure 18 and 19).

g') As a final general remark, may we point out the very large intensity of the transition at ~ 5000 cm^{-1}, especially at room temperature, and the pronounced temperature-dependance of its intensity.

h') Specific remarks on various bands are also given in the figure captions.

Table IV

Energy and composition of J-manifolds for U^{4+}, assuming $\zeta/F_2 = 4{\cdot}73$; $F_4/F_2 = 0{\cdot}1418$; $F_6/F_2 = 1{\cdot}606 \times 10^{-2}$ (see text).

Level	Composition	Energy in F_2 units	Diagonal Crystal-Field energy of Γ_1 levels[a]
$\lvert {}^3H_4' \rangle$	$0{\cdot}9293 \lvert {}^3H_4\rangle - 0{\cdot}3428 \lvert {}^1G_4\rangle + 0{\cdot}1000 \lvert {}^3F_4\rangle$	0	$-1{\cdot}5$
$\lvert {}^3F_2' \rangle$	$0{\cdot}9246 \lvert {}^3F_2\rangle + 0{\cdot}3672 \lvert {}^1D_2\rangle + 0{\cdot}0909 \lvert {}^3P_2\rangle$	19·78	
$\lvert {}^3H_5' \rangle$	$\lvert {}^3H_5\rangle$	30·02	
$\lvert {}^3F_4' \rangle$	$-0{\cdot}3234 \lvert {}^3H_4\rangle - 0{\cdot}6862 \lvert {}^1G_4\rangle + 0{\cdot}6514 \lvert {}^3F_4\rangle$	43·01	$-1{\cdot}02$
$\lvert {}^3F_3' \rangle$	$\lvert {}^3F_3\rangle$	43·17	
$\lvert {}^3H_6' \rangle$	$0{\cdot}9571 \lvert {}^3H_6\rangle - 0{\cdot}2893 \lvert {}^1I_6\rangle$	54·90	$+1{\cdot}0$
$\lvert {}^3P_0' \rangle$	$0{\cdot}956 \lvert {}^3P_0\rangle - 0{\cdot}295 \lvert {}^1S_0\rangle$	76·55	0·0
$\lvert {}^1D_2' \rangle$	$-0{\cdot}3420 \lvert {}^3F_2\rangle + 0{\cdot}7142 \lvert {}^1D_2\rangle + 0{\cdot}6105 \lvert {}^3P_2\rangle$	77·36	
$\lvert {}^1G_4' \rangle$	$0{\cdot}1555 \lvert {}^3H_4\rangle + 0{\cdot}6405 \lvert {}^1G_4\rangle + 0{\cdot}7518 \lvert {}^3F_4\rangle$	77·52	$-1{\cdot}01$
$\lvert {}^3P_1' \rangle$	$\lvert {}^3P_1\rangle$	91·28	
$\lvert {}^1I_6' \rangle$	$0{\cdot}2898 \lvert {}^3H_6\rangle + 0{\cdot}9571 \lvert {}^1I_6\rangle$	96·90	$-1{\cdot}6$
$\lvert {}^3P_2' \rangle$	$0{\cdot}1588 \lvert {}^3F_2\rangle - 0{\cdot}5972 \lvert {}^1D_2\rangle + 0{\cdot}7861 \lvert {}^3P_2\rangle$	116·08	
$\lvert {}^1S_0' \rangle$	$0{\cdot}295 \lvert {}^3P_0\rangle + 0{\cdot}956 \lvert {}^1S_0\rangle$	192·65	0·0

[a]) In units of the parameter A, assuming $B = 4 \times 10^{-2}$ A.

5. The electronic energy-level scheme for U^{4+}

The U^{4+} ion has the electronic configuration (Rn) $5f^2$, the $5f$-electrons being surrounded by the $6s^2\,6p^6$ electronic cloud. The effect of the electrostatic interaction between the two $5f$ electrons, as in the similar case of Pr^{3+}, gives rise to the *terms* ^3H, ^3F, ^1G, ^1D, ^1I, ^3P and ^1S in order of increasing energy.

*) A similar effect, attributed to the formation in solutions of hydrogen bonds, has been reported. (J. L. Ryan, Inorg. Chem. *3*, 211 (1964).

Spin-orbit coupling splits and mixes the terms. New levels are obtained characterized by the quantum number J. Relevant matrices are to be found in SPEDDING[13]) and SATTEN and MARGOLIS[14]); plots of the intermediate-coupling energy-level scheme are given by CONWAY[15]) and JØRGENSEN[16]). In the case of U^{4+}, the spin-orbit coupling constant $\zeta_{5f} \simeq 1800\ cm^{-1}$ is much larger than that for Pr^{3+}, where $\zeta_{4f} \simeq 800\ cm^{-1}$.

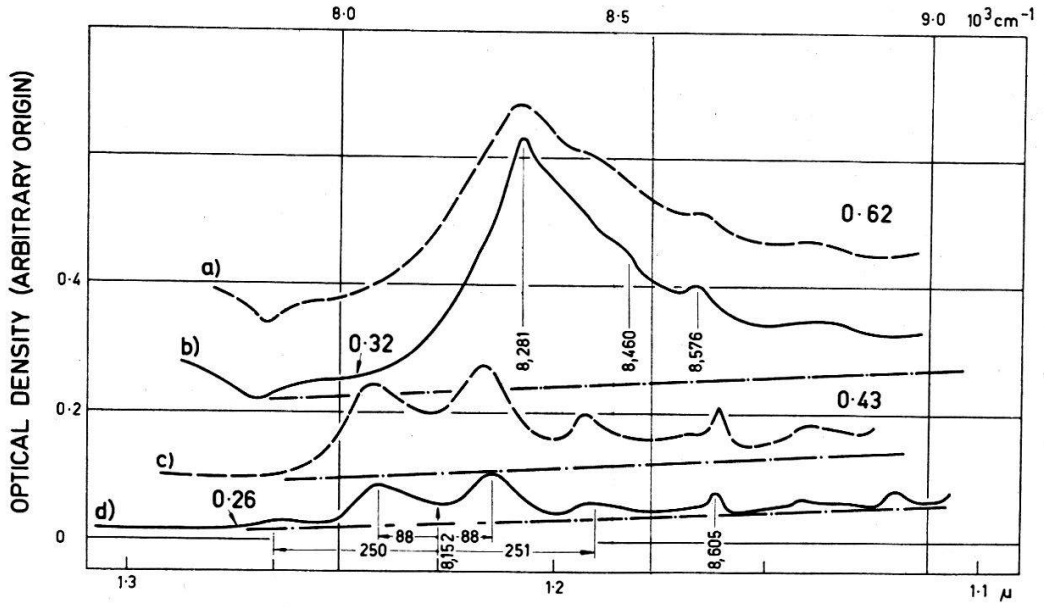

Figure 9

a) $[P\phi_3H]_2\ UCl_6$, sample F6 at RT; b) same at 78° K; c) $[P\phi_3H]_2$ (Sn, U)Cl_6, sample F4 at RT; d) same at 78° K.

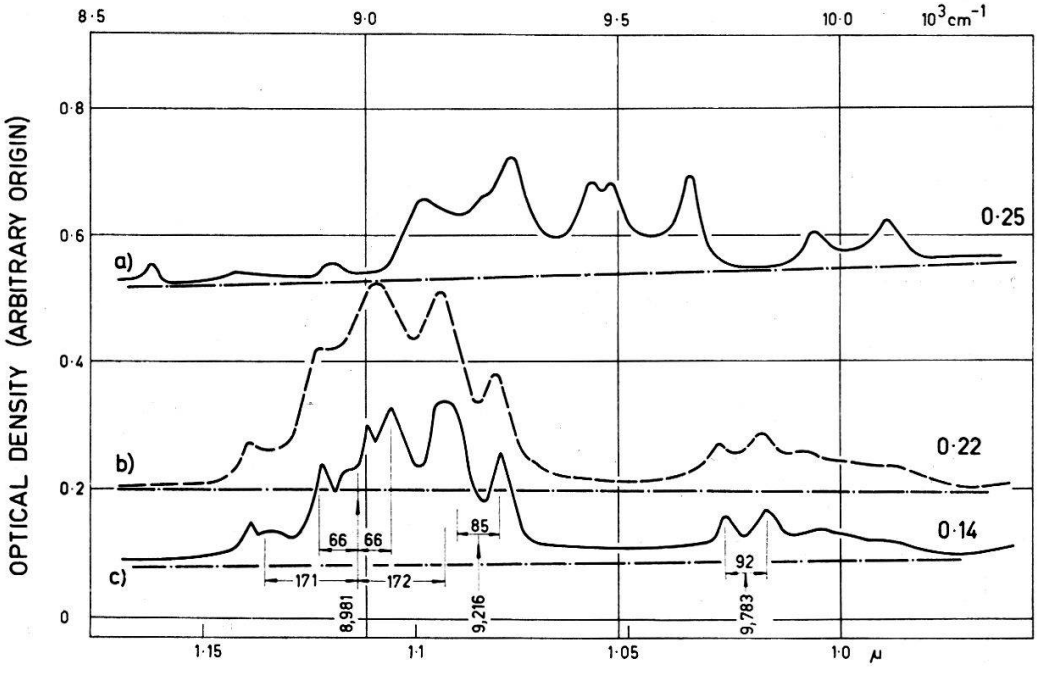

Figure 10

a) $[P\phi_3H]_2$ (Sn, U) Cl_6, sample F4 at 78° K; b) $[P\phi_3H]_2$ (Sn, U)Br_6, sample F5 at RT; c) same at 78° K; Possible analysis of the fine structure of curve c) involving electronic levels (vertical arrows) at 8,981, 9,216 and 9,783 cm^{-1}.

Table IV shows the energy and the composition of the intermediate-coupling levels of U^{4+} for a definite choice of the pertinent parameters. We assumed[17] $F_2 = 190\ cm^{-1}$; $\zeta_{5f} = 1800\ cm^{-1}$: $F_4/F_2 = 0{\cdot}1418$ and $F_6/F_2 = 1{\cdot}606 \times 10^{-2}$. The latter ratios do not differ greatly from the ratios of the F_k parameters for hydrogenic $5f$-functions, that is $F_4/F_2 = 0{\cdot}145$ and $F_6/F_2 = 1{\cdot}64 \times 10^{-2}$, as given by ELLIOTT, JUDD and RUNCIMAN[18]).

When the U^{4+} ion is surrounded by an octahedron of chlorines or bromines, then the energy levels of $5f^2$ are derived from the splitting and mixing of the J-manifolds and will be labelled by the cubic-symmetry representations Γ's. The number of cubic-symmetry levels obtained from each J-manifold can be found in BETHE[19]). The matrices for f^2-systems in cubic fields, inclusive of crystal-field mixing of various J-levels have been given by SATTEN and MARGOLIS[14]). Since f-electrons are involved, the crystal-field splitting will depend on two parameters, namely a scale factor A for the 4th degree cubic-symmetry potential, and the scale factor B for the 6th degree cubic-symmetry potential.

This implies that the position of the elctronic levels of the system generally will depend on 6 parameters, namely the F_2, F_4, F_6 parameters, the spin-orbit coupling

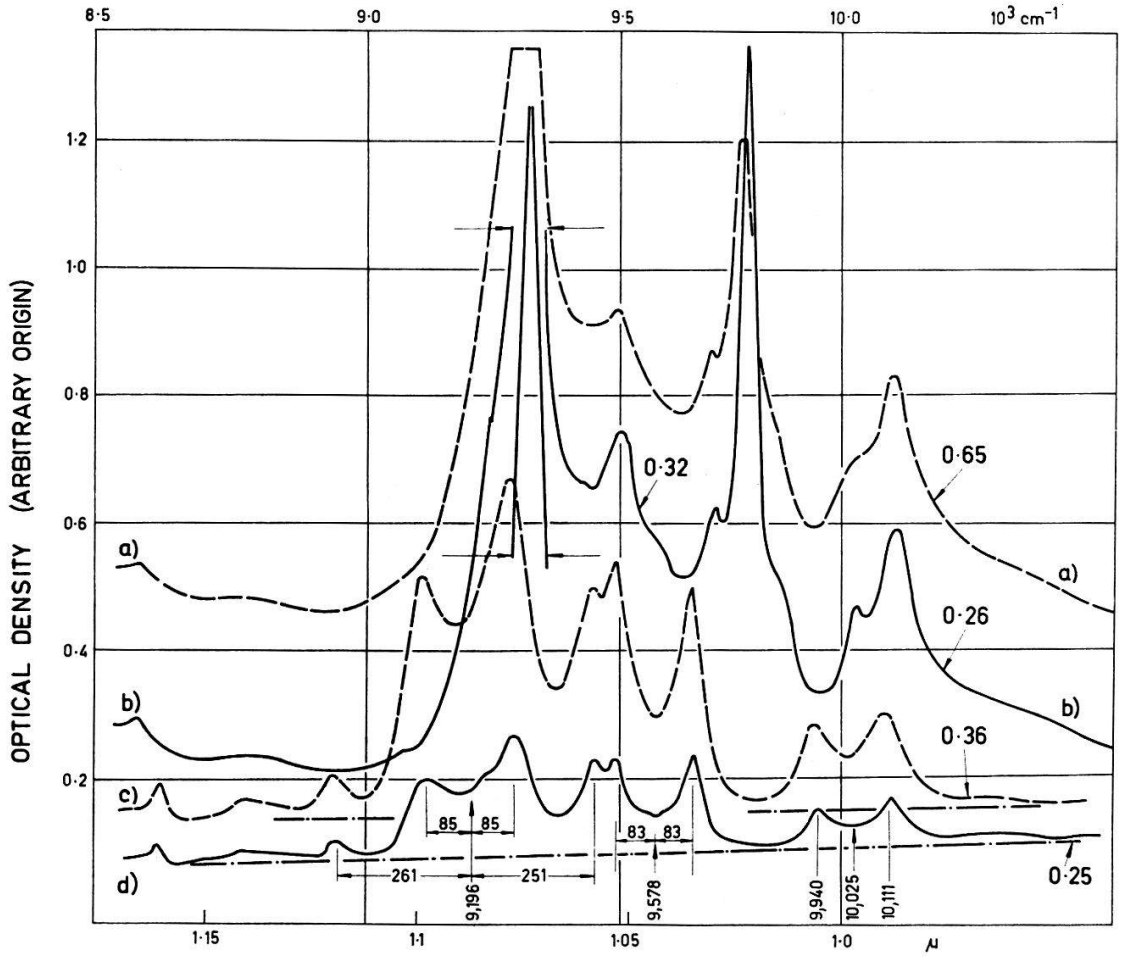

Figure 11

a) $[P\phi_3H]_2\ UCl_6$, sample F6 at RT; b) same at 78° K; c) $[P\phi_3H]_2$ (Sn, U)Cl_6, sample F4 at RT; d) same at 78° K. Vertical arrow indicate position of 'pure' electronic transitions.

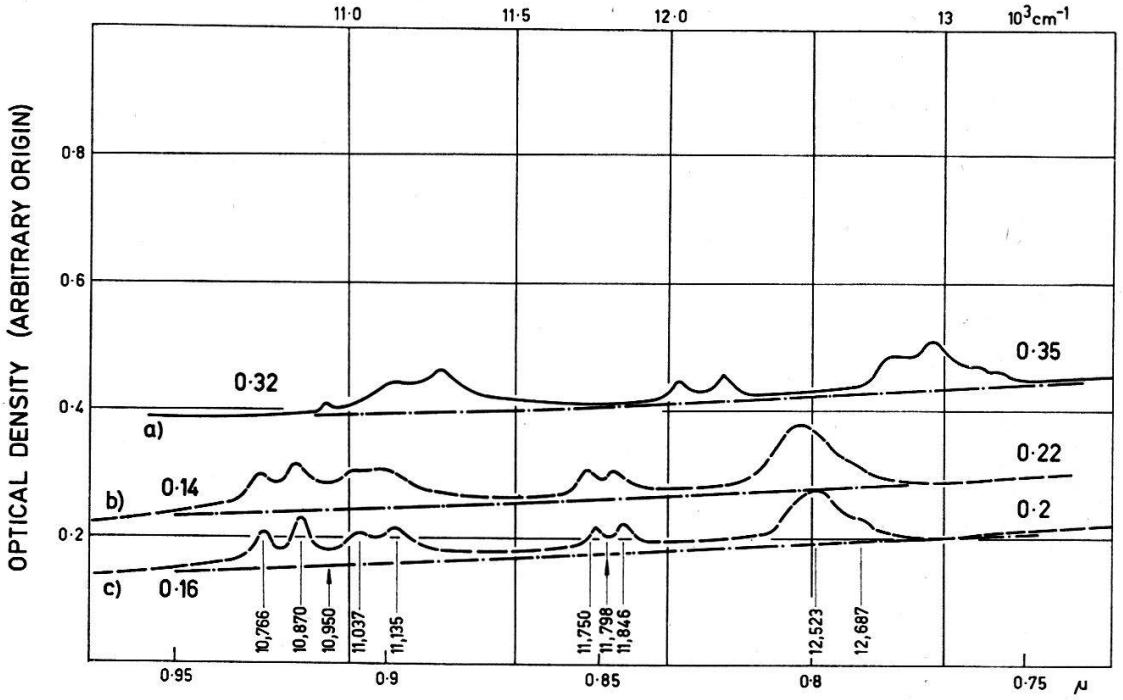

Figure 12

a) $[P\phi_3H]_2$ (U, Sn)Cl_6, sample F4 at 78° K; b) $[P\phi_3H]_2$ (U, Sn)Br_6, sample F5 at RT; c) same at 78° K.

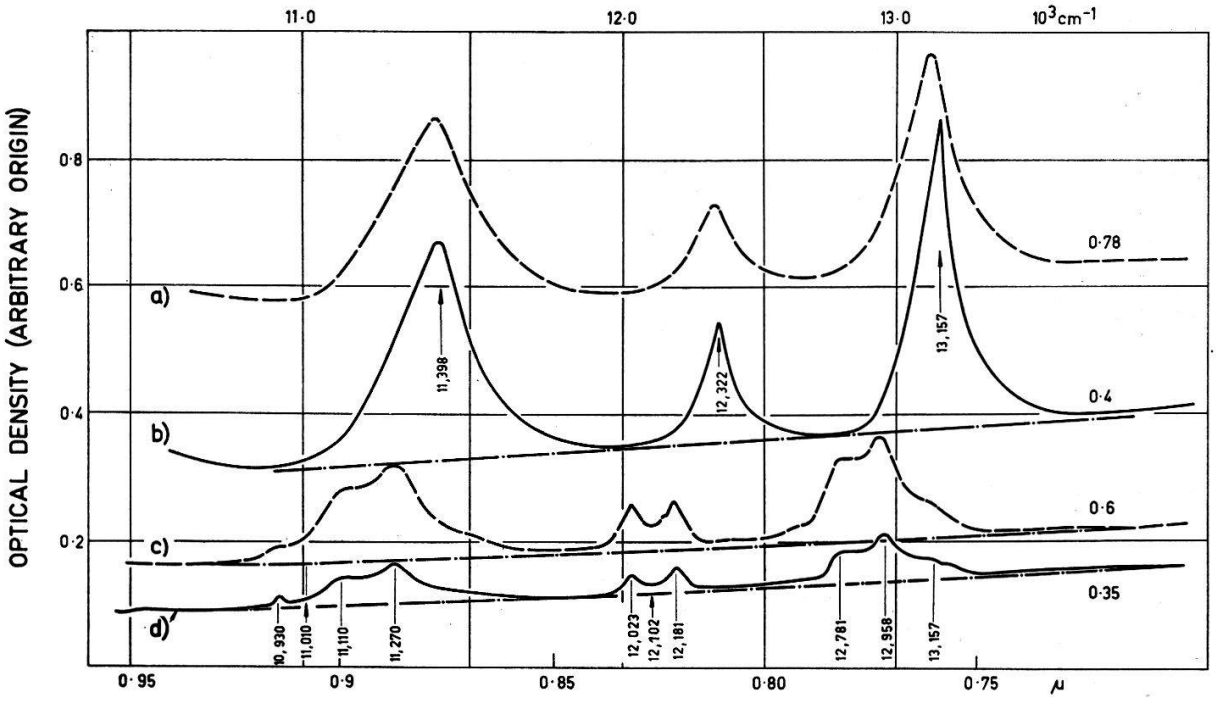

Figure 13

a) $[P\phi_3H]_2$ UCl_6, sample F6 at RT; b) same at 78° K; c) $[P\phi_3H]_2$ (Sn, U)Cl_6, sample F4 at RT; d) same at 78° K. The sharp spikes and the absence of structure for curve b) suggest the transition to be the 'pure' electronic ones. Vertical arrows in b) and d) indicate 'pure' electronic transitions.

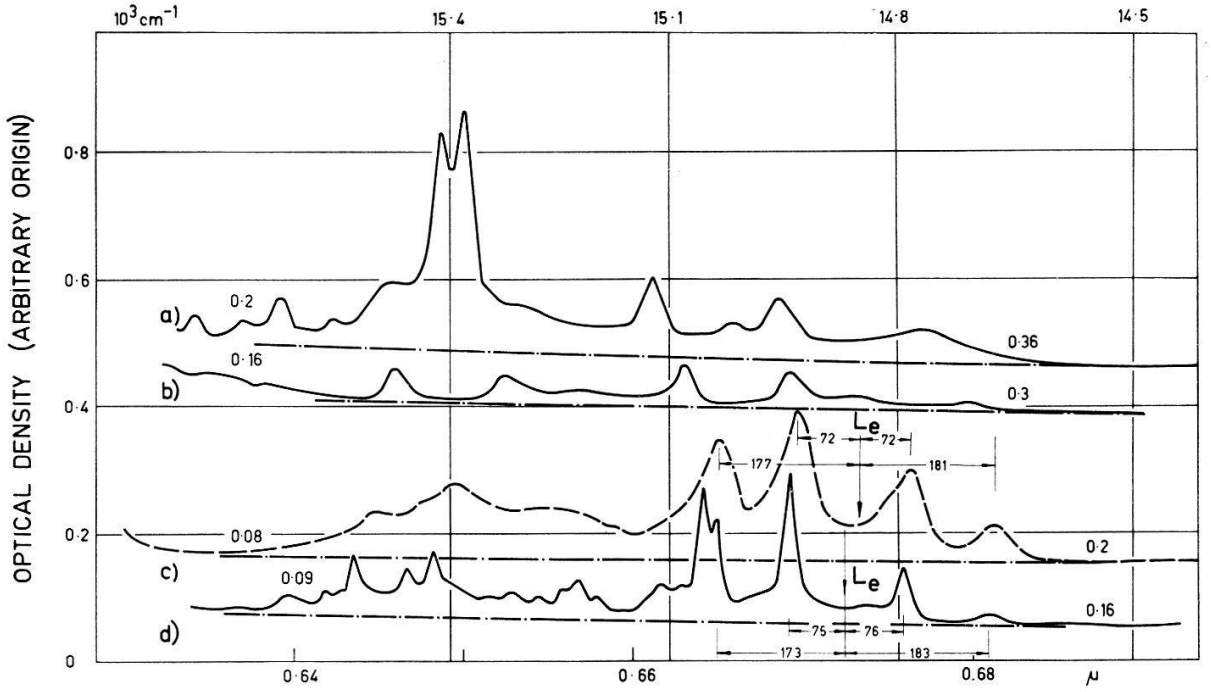

Figure 14

a) $[P\phi_3H]_2 UCl_6$, sample F6 at 78° K; b) $[P\phi_3H]_2$ (Sn, U)Cl_6, sample F4 at 78° K; c) $[P\phi_3H]_2 \cdot$ (Sn, U)Br_6, sample F5 at RT; d) same at 78° K. Positive temperature shift of L_e (~ 8 cm^{-1}) (For this figure and the following ones the direction of scanning is inverted).

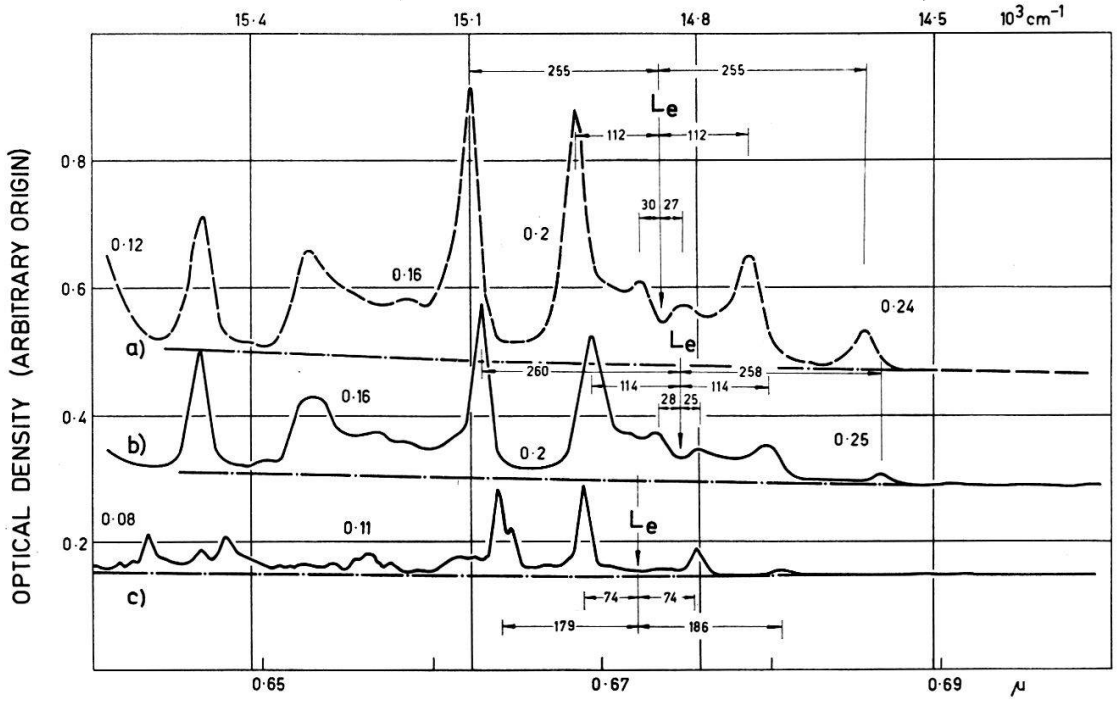

Figure 15

a) $[P\phi_3H]_2$ (Sn, U)Cl_6, sample B3; 1 mm thick. Room Temperat.; b) same at 78° K; c) $[P\phi_3H]_2 \cdot$ (Sn, U)Br_6, sample B2; 0·5 mm thick. Temp. 78° K; L_e ('pure' electronic transition) for a) is at 14,846 cm^{-1}, while for b) at 14, 824, that is it has a negative temperature shift. Notice the absence of Γ_{5u} vibration of 80 cm^{-1}. L_e for c) is located at 14,876 cm^{-1}. Note in c) the splitting of the peak at $\sim$ 15,100 cm^{-1}. Such splitting is absent in the undiluted $[P\phi_3H]_2 UBr_6$ salt (Figure 17a).

constant ζ_{5f} and the crystal field parameters A and B. The f^2-system in cubic-symmetry has seven Γ_1 levels, three Γ_2, nine Γ_3, nine Γ_4, twelve Γ_5 levels. There is a large enough number of levels to check the consistency of any choice of the six parameters mentioned above. The work by SATTEN and alii has been of very great value in showing that a very large number of the observed absorption lines U^{4+} are of vibronic nature, and that from the absence of some of the intense vibronic lines one can have clues as to the symmetry properties of the related electronic level [see (1); (2)]. Finally the temperature shifts of the electronic lines can give indication of the relative slope of the energy plots *v s* crystal field strength for the ground and excited levels.

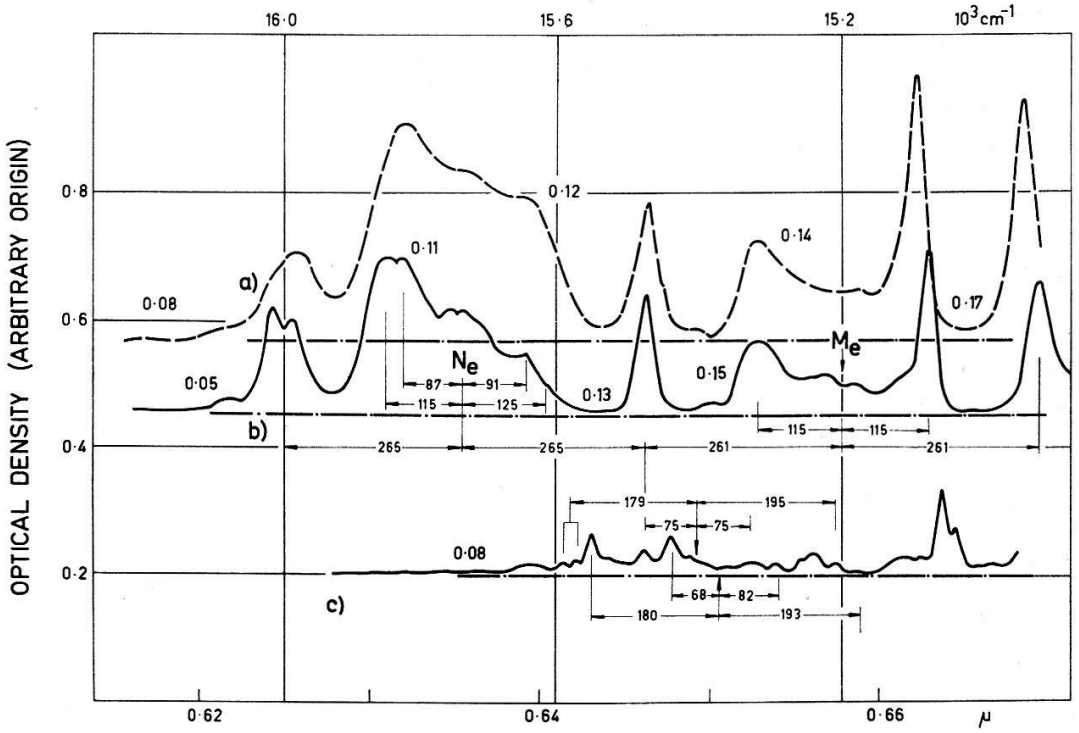

Figure 16

a) $[P\phi_3H]_2$ (U, Sn)Cl_6, sample B3 at RT; b) same at 78° K; c) $[P\phi_3H]_2$ (U, Sn)Br_6, sample B2 at 78° K. The electronic transitions of curve b) are located at 15,200 cm^{-1} (M_e) and 15,735 cm^{-1} (N_e). Note in curve b) the splitting of the peak at $\sim$ 16,000 cm^{-1} and the anomalous temperature behaviour of the peak at $\sim$ 15,500 cm^{-1}, which does not shift in position or change in intensity from a) to b). If the analysis of curve b) is correct, the negative temperature shift of L_e could be due *in part* to the intensity decrease of the longwavelength components of group M (see Figure 15). In curve c) a possible analysis of the complex fine structure in terms of two electronic levels at 15,368 cm^{-1} and 15,400 cm^{-1} is indicated.

6. The magnitude of the crystal field

The main problem in the preliminary interpretation of the $5f^n$ spectra still is that of making a suitable assumption as to the magnitude of the crystal-field parameters, that is, in general, are the $5f^n$ spectra characterized by a small crystal-field as the $4f^n$ system, or is this field one or two orders of magnitude larger?

CONWAY[15]) interpreted his data on the $CaF_2 + UF_4$ system on the basis of a weak crystal-field. Unfortunately no details of his spectra are published. Against this, the following reasons point to a large crystal-field in U^{4+}.

a) Magnetic susceptibility studies[12]) indicate that $^3H_4$ is split by a cubic crystal field in such a way that the ground level is $^3H_4$ (Γ_1) and that no electronic levels are situated close enough to the ground level to give a strong temperature-dependent contribution to the magnetic susceptibility.

b) If the crystal field was weak, a clustering of Stark levels arising from the splitting of the free-ion J-levels should be the common pattern of the spectrum. This does not seem to happen (Compare Table II and Table IV).

c) The large red shift in the spectrum of $\langle UBr_6\rangle^{2-}$ when compared to that of $\langle UCl_6\rangle^{2-}$. Although in the case of the rare earths one has similar shifts, they are much smaller than those listed in Table III. RICHMAN and WONG[20]) give red shifts ranging from 10 cm^{-1} to 150 cm^{-1} in the case of $LaBr_3 : Nd^{3+}$, compared with $LaCl_3 : Nd^{3+}$.

d) In the case of a weak crystal field, mixing of the various J levels would not be important, and only the diagonal energy of the crystal-field would be significant. Then from Table IV, column 4, the level $^3F'_4$ (Γ_1) should show the same peculiar

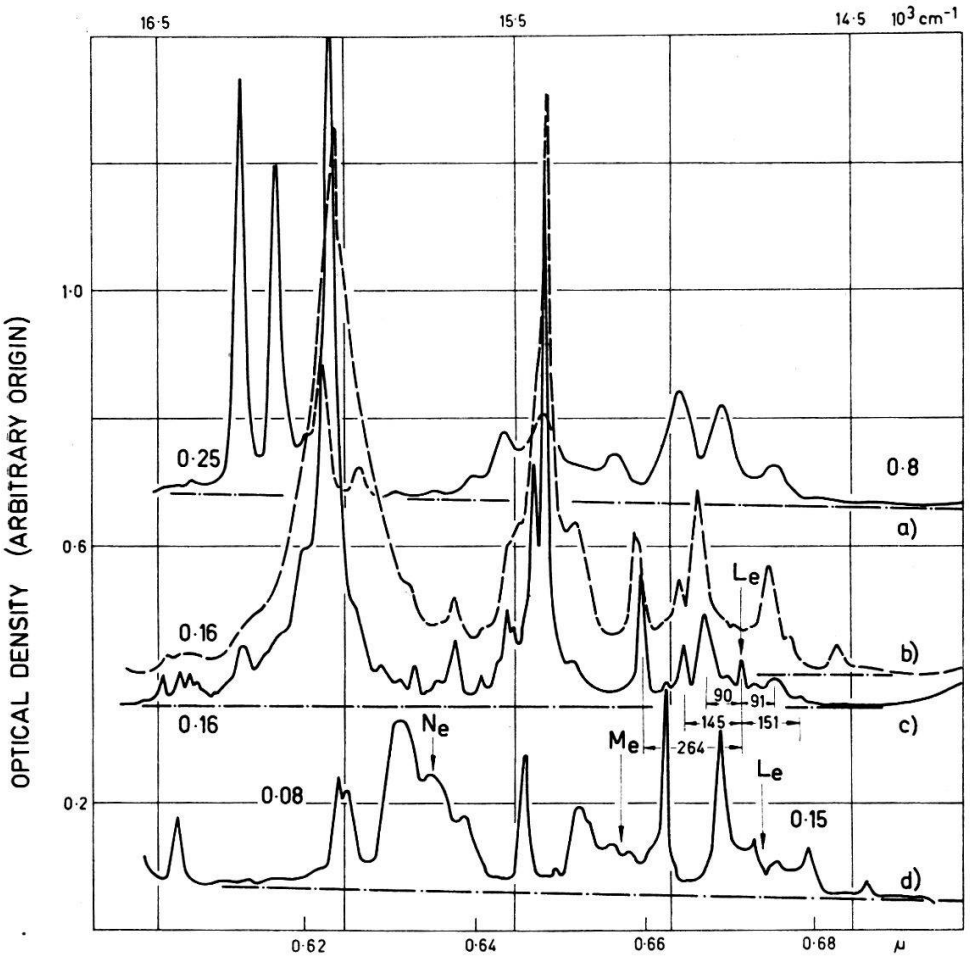

Figure 17

a) Undiluted $[P\phi_3H]_2\,UBr_6$, sample A1 (1 mm thick) at 78° K; b) Undiluted $[P\phi_3H]_2\,UCl_6$, sample A3 (0·95 mm thick) at RT; c) same at 78° K; d) $[P\phi_3H]_2$ (Sn, U)Cl_6, sample B3, at 78° K. The third peak of group L in a) does not show the splitting of the corresponding tin-diluted crystal (Figure 14). This is probably due to the large slit-width. Transition L_e is present for $[P\phi_3H]_2\,UCl_6$ at 78° K (curve c)). The group L shows a negative temperature shift (curve b) and c)). L_e at 14,905 cm^{-1} at RT and at 14,892 cm^{-1} for 78° K.

behaviour as the group G_4' (Γ_1), we associated to the L_e transition (Table IV), that is negative temperature behaviour in the chloride and absence of red shift from the chloride to the bromide complex. This behaviour is not observed.

A large crystal-field mixing for various J-levels implies that the energy of the Γ levels are obtained from the solution of secular equations of 7^{th}; 3^{rd}; 9^{th}, and 12^{th} degree for Γ_1, Γ_2, Γ_3, Γ_4 and Γ_5 respectively. An attempt to solve the secular equation for Γ_1 levels using second order perturbation techniques fails because the energy separation of the unperturbed levels have the same order of magnitude as the square of the non-diagonal matrix elements.

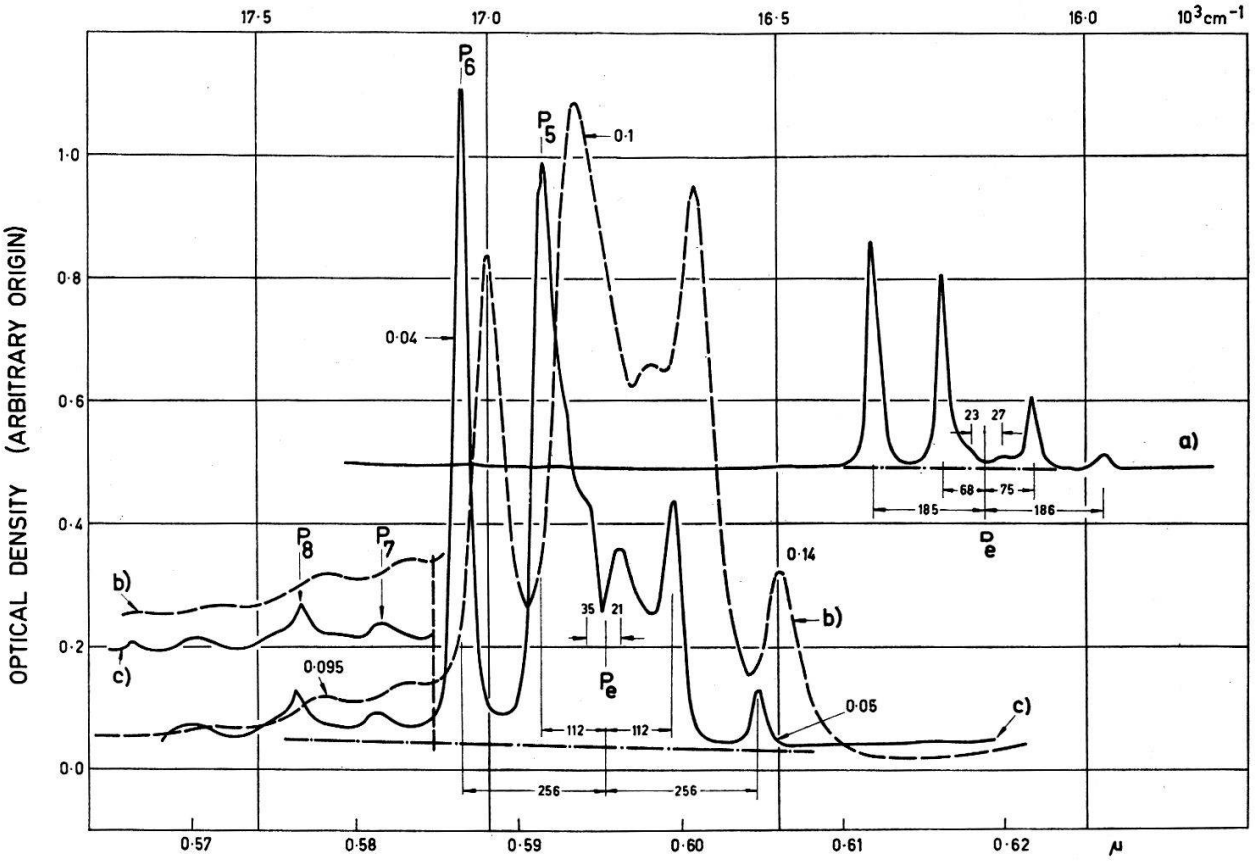

Figure 18

a) [P ϕ_3H_2 (Sn, U)Br_6, sample B2 at 78° K. Electronic transition P_e at 16,159 cm^{-1}. The most intense peak is asymmetric, possibly a doublet, as for the group L. Some low-frequency vibrations ($\sim$ 25 cm^{-1}) seem to be present. b) [P $\phi_3H]_2$ (Sn, U)Cl_6, sample B3 at RT. c) same at 78° K. The electronic level P_e is located at 16,790 cm^{-1} (curve c)). The temperature shift of the lines corresponding to ν (256) is very pronounced, 41 cm^{-1}. The tails of curve b) and e) have been repeated on a shifted base-line, for better comparison. The separation P_8–P_7 = 146 cm^{-1} compares favourably with the separation P_6–P_5 = 144 cm^{-1}. SATTEN et alii[7][8]) list a large number of lines corresponding to combination frequencies.

7. Qualitative considerations on the observed spectra

Since Professor R. SATTEN and Dr. SCHREIBER intend to make a complete comparison between MARGOLIS and SATTEN's determinants for f^2 in octahedral symmetry[14]) and the electronic levels observed in salts of UCl_6^{2-}, we are not attempting

such an analysis. However, we may point out a few striking general features: If the ligand field parameters have the same order of magnitude as in AXE's study[21]) of Pa(IV) in Cs_2ZrCl_6, that is A $\sim$ 1000 cm^{-1} and B $\sim$ 40 cm^{-1}, then most J-levels of the configuration 5 f^2 are only distributed over some 1000 to 2000 cm^{-1} with respect to the components of well-defined cubic symmetry type Γ_n. Thus, the ground state is the temperature-independent paramagnetic component Γ_1 of $^3H_4$. The component Γ_4 follows at 910 cm^{-1}, the transition from the ground state being permitted as magnetic dipole radiation[22]). The energy of the two other components of $^3H_4$, Γ_3 and Γ_5 is slightly higher.

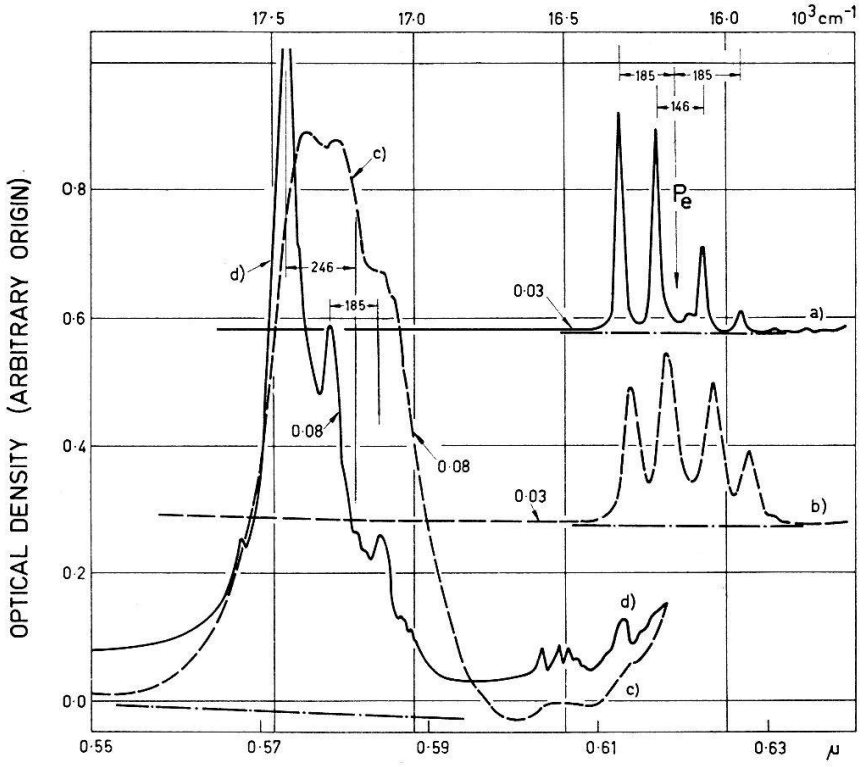

Figure 19

a) $[P\phi_3H]_2$ (Sn, U)Br_6, sample B2 at 78° K; b) same at RT. Positive temperature shift of group P. c) $[P\phi_3H]_2$ UCl_6 sample A3 at RT; d) same at 78° K. Electronic level at 17,205 cm^{-1} (curve d). Structurally the groups of curve a) and d) are similar.

Regarding the excited J-levels, we will make the simplifying assumption that the six appropriate parameters fall into two classes, one pertaining to the central field of spherical symmetry (E^1, E^2 and E^3 for inter-electronic repulsion, or other linear combinations, such as F_2, F_4 and F_6; and the Landé parameter $\zeta_{f,p}$) and one pertaining to the perturbations of essential octahedral symmetry (the M. O. energy differences[23]) Δ and Θ, or their linear combinations A and B already mentioned). When comparing UCl_6^{2-} with UBr_6^{2-}, or comparing the same complex ion at two different temperatures, we apply the approximation that each of these two classes vary with a characteristic multiplicative factor; let us call them β for the spherical and δ for the 'ligand field' parameters. We expect the results to be:

$UCl_6^{2-} \rightarrow UBr_6^{2-}$	$300° K \rightarrow 77° K$	
β decreases some 4%	β decreases very slightly	
δ decreases some 10%	δ increases slightly	(7)

The arguments for the expected difference between the chloro and bromo complexes are based on the behaviour of the other transition groups[3)24)] and are confirmed by a comparison of UBr_6^{2-} and UI_6^{2-} in acetonitrile solution[25)]. The temperature effect

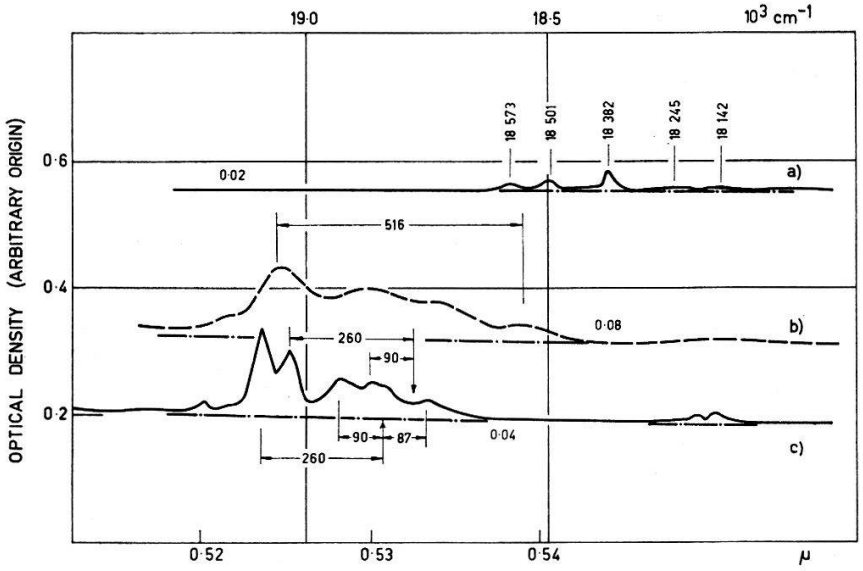

Figure 20

a) $[P\phi_3H]_2$ (Sn, U)Br_6 sample B2, at 78° K. The same group is shown in the next figure, for a more absorbing sample and at higher scanning speed. b) $[P\phi_3H]_2$ (Sn, U)Cl_6 sample B3 at RT. c) Same at 78° K. Two possible electronic levels at 18,776 and 18,838 cm^{-1}. The weak doublet on the right of curve c) is probably an overtone of group *P*.

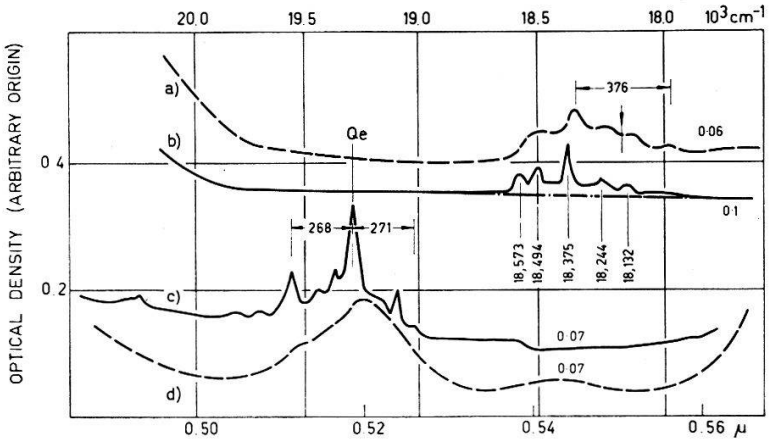

Figure 21

a) $[P\phi_3H]_2$ UBr_6, sample A1 at RT; b) same at 78° K; c) $[P\phi_3H]_2$ UCl_6, sample A3 at 78° K; d) same at RT. Vertical arrow on a) gives estimate of one electronic transition ($\sim$ 18,160 cm^{-1}). In curve c) Q_e at 19,286 cm^{-1} seems to be the corresponding electronic level.

is expected to be comparable to the effect of 100,000 atmospheres pressure[26][27]). Hence, going from UCl_6^{2-} to UBr_6^{2-}, we would expect the width of each J-group to decrease (because it is roughly proportional to δ) and the baricenter of each group to shift to lower wavenumbers (because this wavenumber mainly is represented by the nephelauxetic ratio β). In other words, each group of electronic Γ_n levels corresponding to one (or two adjacent) J-level should show a shift to smaller wavenumbers, much larger at the 'blue' end of a given group (because the decrease of β and δ cooperate) than at the 'red' end of a given group. In the case of the first Γ_n component of a given

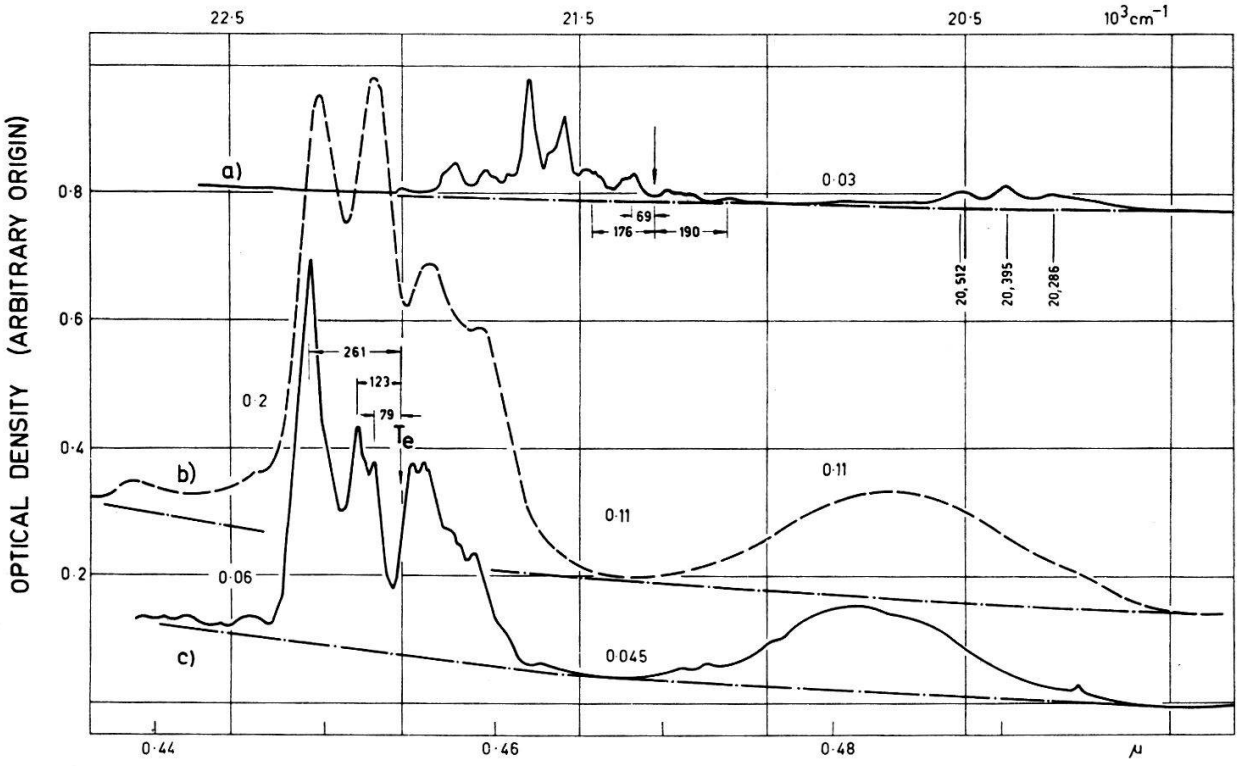

Figure 22

a) $[P\phi_3H]_2$ (Sn, U)Br_6, sample B2 at 78° K. One electronic level estimated at 21,297 cm^{-1}
b) $[P\phi_3H]_2$ (Sn, U)Cl_6, sample B3 at RT; c) same at 78° K. At least one electronic level, T_e is located at 22,000 cm^{-1}.

J-group, it is even conceivable that the decrease of δ cancels the effects of decreased β, and one observes a comparable wavenumber for the two complexes. Actually, such stationary Γ_n levels are found each time as the first member of a group of adjacent levels (group G, H, L, M, S, T) and a most extreme example in the group L, the first Γ_n level in the red, shifting to *higher* wavenumber in UBr_6^{2-}. Already SATTEN, YOUNG and GRUEN[7]) reported in chloride complexes the opposite temperature shift of this group which can be rationalized if it is the Γ_1 component of $^1G_4$ (heavily mixed with $^3F_4$) which is one of the few levels varying equally much in the direction of lower energy as function of increasing δ as the groundstate. An alternative explanation assuming slightly different spherical parameters, is that the transition in question is Γ_1 of the $^3P_1$ level. In this case, it has a rather mixed J-value, due to the non-diagonal elements of the Margolis-Satten determinants[14]).

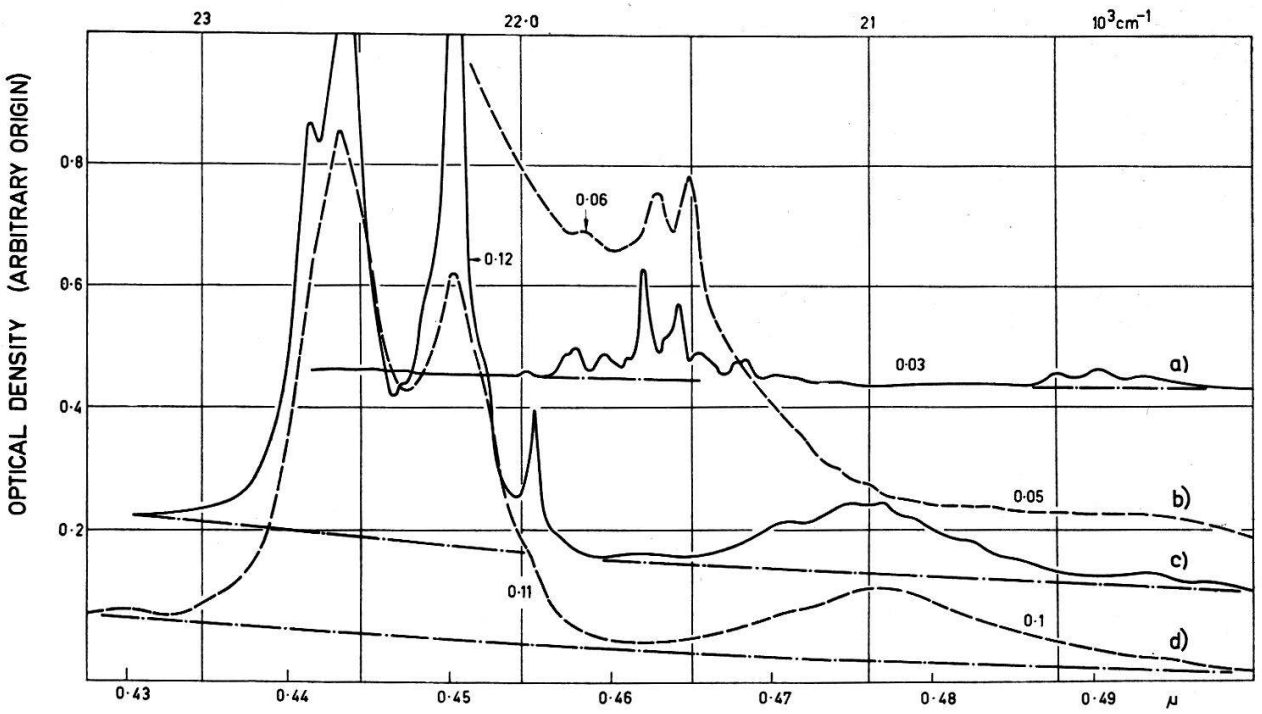

Figure 23

a) $[P\phi_3H]_2$ (Sn, U)Br_6, sample B2 at 78° K; b) same at RT. Sample J4, 0·8 mm thick. The steep continuous absorption of curve a) is only found in Sn-containing crystals, and shifts to higher energies at low temperatures. c) $[P\phi_3H]_2UCl_6$ sample A4, 0·75 mm thick. Temp. 78° K. d) same at RT.

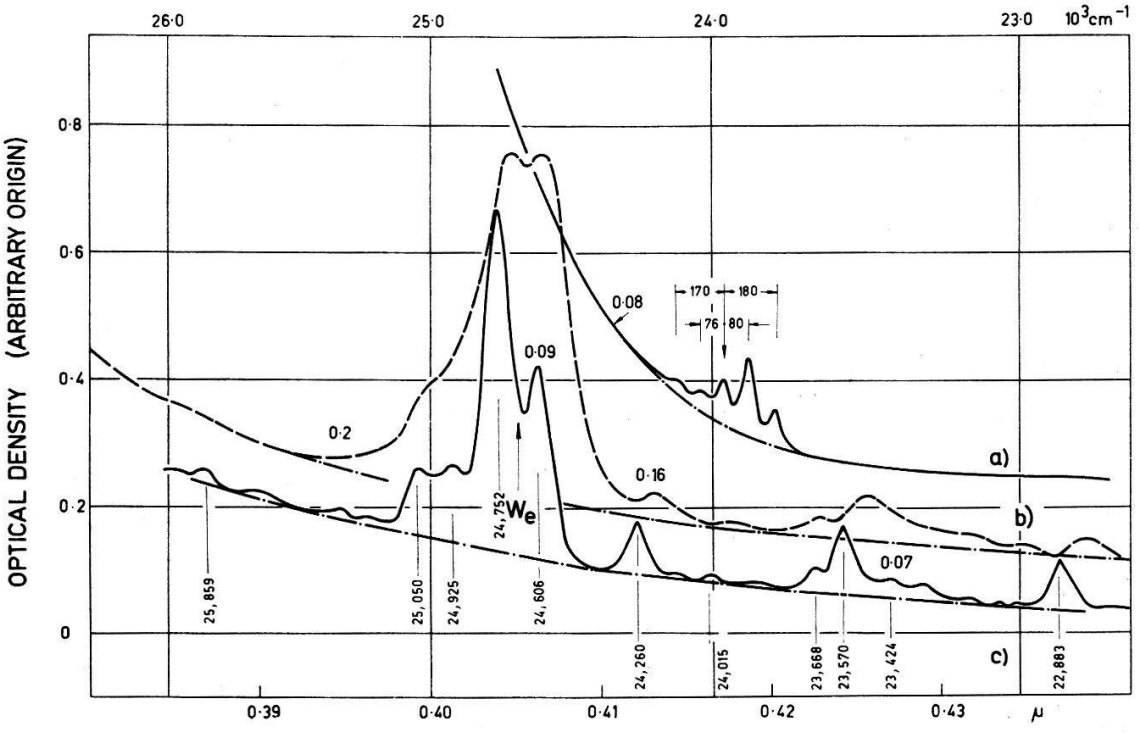

Figure 24

a) $[P\phi_3H]_2$ (Sn, U) Br_6, sample B2 at 78° K. Possible electronic level at 23,960 cm^{-1}. b) $[P\phi_3H]_2$ (Sn, U)Cl_6, sample B3 at RT. c) Same at 78° K. W_e at ~ 24,680 cm^{-1}.

The stabilization of the Γ_1-groundstate in UCl_6^{2-} relative to UBr_6^{2-} is proportional to δ but it is only expected to be some 5% of the total width of the $^3H_4$ group, i.e. some 100 cm^{-1}. This contributes to the apparent larger value of β in UCl_6^{2-} compared with UBr_6^{2-} because all excited levels are shifted to higher wavenumber in the chloride. However, it is a rather minor effect compared with the manifest decrease of β producing band shifts as large as 800 cm^{-1} in the blue (e.g. the intense groups T and W). It is worth noting that the individual J-baricenters are shifted slightly differently (Table III). Though the nephelauxetic effect is ten times stronger in $U(IV)X_6^{2-}$ than in Nd(III) in LaX_3, the study of Nd(III) in $LaBr_3$ reveals a similar scattering of the actual β values[20]).

Riassunto. Spettri di assorbimento ottico di cristalli contenenti U^{4+} a coordinazione ottaedrica in sali complessi di trifenilfosfonio sono stati studiati a temperatura ambiente e a 78° K, nella regione da 2.5 μ sino a 0.3 μ. Frequenze di vibrazione dei gruppi $\langle UCl_6\rangle^{2-}$ e $\langle UBr_6\rangle^{2-}$ sono presenti in assorbimento, sovrapposte alle transizioni elettroniche. Le proprietà generali degli spettri in questione sono discusse in relazione ai livelli elettronici del sistema $5f^2$.

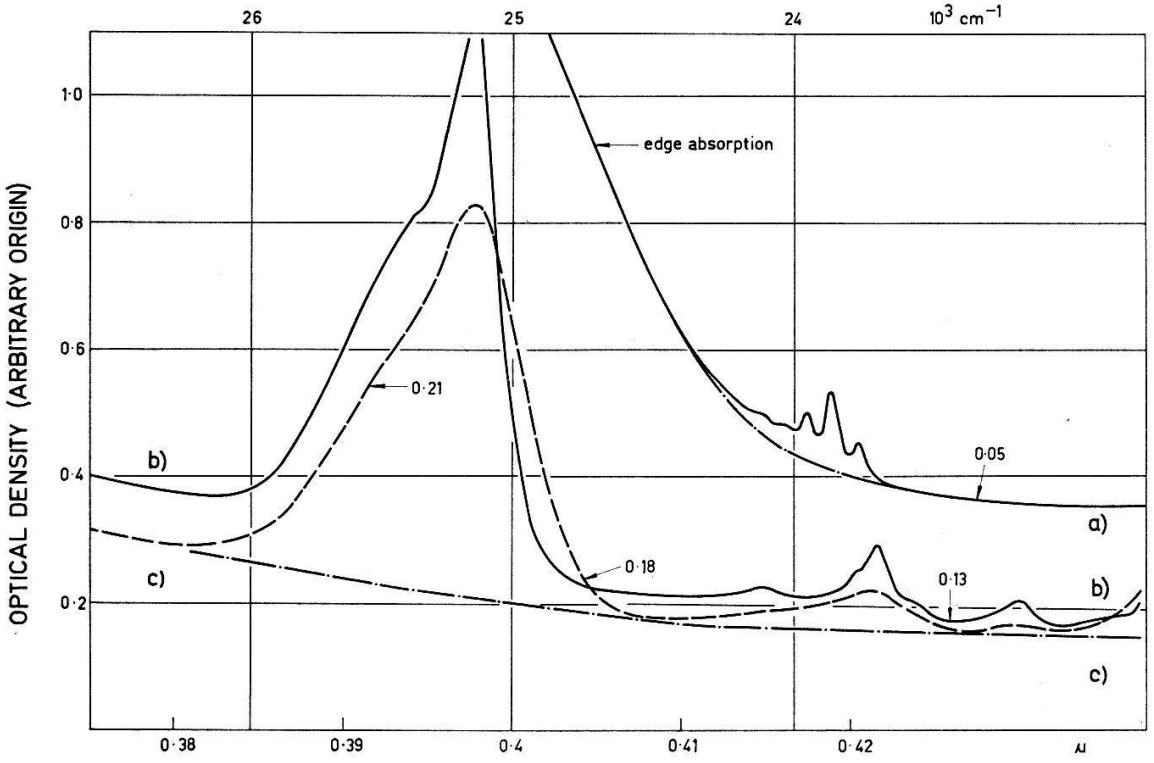

Figure 25

a) $[P\phi_3H]_2$ (Sn, U)Br_6, sample B2, Temp. 78° K; b) $[P\phi_3H]_2UCl_6$, sample A4, Temp. 78° K; c) same at RT.

Acknowledgements

We would like to thank Dr. L. Venanzi of Oxford University and Dr. R. A. Satten of the University of California for stimulating discussions on the problem.

Appreciation is due to Mr. S. Losi and G. Casaro for technical assistance; to Mrs. E. Schneider for making drawings of the photometric curves and Miss M. L. Bischoff for secretarial assistance.

References

[1]) Y. TANABE and S. SUGANO, J. Phys. Soc. Jap. *9*, 753–766 (1954).
[2]) D. S. MCCLURE, Solid State Physics *9*, 399 (1959).
[3]) C. K. JØRGENSEN, Absorption Spectra and Chemical Bonding in Complexes. Pergamon Press, 1962. (U.S. distributor: Addison-Wesley, Reading, Mass.)
[4]) W. A. RUNCIMAN, Rept. Progr. Phys. *21*, 30 (1958).
[5]) Ref. 3, Page 173–190.
[6]) C. K. JØRGENSEN, Mol. Phys. *2*, 96 (1956).
[7]) R. A. SATTEN, D. J. YOUNG and D. M. GRUEN, J. Chem. Phys. *33*, 1140 (1960).
[8]) S. A. POLLACK and R. A. SATTEN, J. Chem. Phys., *36*, 804 (1962).
[9]) L. VENANZI and PH. DAY, private communication.
[10]) J. A. C. ALLISON and F. G. MANN, J. Chem. Soc. 2915 (1949).
[11]) C. K. JØRGENSEN, Acta Chem. Scand. *17*, 251 (1963).
[12]) C. HUTCHISON and G. CANDELA, J. Chem. Phys. *27*, 707 (1957).
[13]) F. H. SPEDDING, Phys. Rev. *58*, 255 (1940).
[14]) R. A. SATTEN and J. MARGOLIS, J. Chem. Phys. *32*, 573 (1960); Erratum J. Chem. Phys. *33*, 618 (1960).
[15]) J. G. CONWAY, J. Chem. Phys. *31*, 1002 (1959).
[16]) Ref. 3, page 178.
[17]) R. A. SATTEN and C. SCHREIBER, private communication.
[18]) J. P. ELLIOTT, B. R. JUDD and W. A. RUNCIMAN, Proc. Roy. Soc., London, *A 240*, 509 (1957).
[19]) H. BETHE, Ann. Physik. *3*, 133 (1929).
[20]) J. RICHMAN and E. Y. WONG, J. Chem. Phys. *37*, 2270 (1962).
[21]) J. D. AXE, Thesis Berkeley UCRL-9293 July 1960.
[22]) R. A. SATTEN, private communication.
[23]) C. K. JØRGENSEN, Orbitals in Atoms and Molecules, page 156, Academic Press 1962, London.
[24]) C. K. JØRGENSEN, Advances Chem. Phys. *5*, 33 (1963).
[25]) J. L. RYAN and C. K. JØRGENSEN, Mol. Phys. *7*, 17 (1963).
[26]) K. B. KEATING and H. G. DRICKAMER, J. Chem. Phys. *34*, 140 (1961).
[27]) H. G. DRICKAMER and J. C. ZAHNER, Adv. Chem. Phys. *4*, 161 (1962).